DEVELOPMENT OF DESIGN EQUATIONS TO ESTIMATE LIVE LOAD EFFECTS IN HAMMER-HEAD BRIDGE PIERS

A THESIS SUBMITTED TO
THE GRADUATE SCHOOL OF NATURAL AND APPLIED SCIENCES
OF
MIDDLE EAST TECHNICAL UNIVERSITY

BY

ÇAĞRI DEMIR

IN PARTIAL FULFILLMENT OF THE REQUIREMENTS
FOR
THE DEGREE OF MASTER OF SCIENCE
IN
ENGINEERING SCIENCES

SEPTEMBER 2019

Approval of the thesis:

DEVELOPMENT OF DESIGN EQUATIONS TO ESTIMATE LIVE LOAD EFFECTS IN HAMMER-HEAD BRIDGE PIERS

submitted by **ÇAĞRI DEMIR** in partial fulfillment of the requirements for the degree of **Master of Science in Engineering Sciences Department, Middle East Technical University** by,

Prof. Dr. Halil Kalıpçılar
Dean, Graduate School of **Natural and Applied Sciences** _____

Prof. Dr. Murat Dicleli
Head of Department, **Engineering Sciences** _____

Prof. Dr. Murat Dicleli
Supervisor, **Engineering Sciences, METU** _____

Examining Committee Members:

Prof. Dr. Murat Altuğ Erberik
Civil Engineering, METU _____

Prof. Dr. Murat Dicleli
Engineering Sciences, METU _____

Prof. Dr. Tolga Akış
Civil Engineering, Atılım University _____

Date: 13.09.2019

I hereby declare that all information in this document has been obtained and presented in accordance with academic rules and ethical conduct. I also declare that, as required by these rules and conduct, I have fully cited and referenced all material and results that are not original to this work.

Name, Surname: Çağrı Demir

Signature:

ABSTRACT

DEVELOPMENT OF DESIGN EQUATIONS TO ESTIMATE LIVE LOAD EFFECTS IN HAMMER-HEAD BRIDGE PIERS

Demir, Çağrı
Master of Science, Engineering Sciences
Supervisor: Prof. Dr. Murat Dicleli

September 2019, 58 pages

In this study, design equations are proposed to calculate the internal forces in hammer-head bridge pier components under the effect of live loads. For this purpose, first a four span benchmark bridge representative of the bridges in the US is selected. Finite element model (FEM) of a benchmark bridge is built, and sensitivity analyses are performed on the bridge model to identify the bridge parameters affecting the magnitude and distribution of the girder live load support reactions and hence the internal forces in the hammer-head pier components. The sensitivity analyses revealed that the number of girders, girder spacing, girder type, slab thickness and the overhang distance significantly affect the magnitude and distribution of the girder live load support reactions and hence the forces in hammer-head pier components. Next, parametric analyses of bridges are performed based on the sensitivity analyses results where each parameter is assigned a wide range of values. Subsequently, minimum least squares regression analyses of more than 50000 data is performed to obtain equations to estimate the maximum cap beam moment and shear force, the maximum column moment and accompanying axial load as well as the maximum column axial load and accompanying moment. The hammer-head pier forces calculated using the

design equations are shown to be in reasonably good agreement with FEM analyses results.

Keywords: Hammer-head pier, live load distribution, design, finite element model

ÖZ

ÇEKİÇ BAŞLI KÖPRÜ AYAKLARINDA HAREKETLİ YÜK ETKİLERİNİN BELİRLENMESİ İÇİN TASARIM DENKLEMLERİNİN GELİŞTİRİLMESİ

Demir, Çağrı
Yüksek Lisans, Mühendislik Bilimleri
Tez Danışmanı: Prof. Dr. Murat Dicleli

Eylül 2019, 58 sayfa

Bu çalışmada, hareketli yük tesirleri altında çekiç başlı köprü ayaklarında oluşan iç kuvvetlerin hesaplanabilmesi için denklemler önerilmiştir. Bu amaçla, öncelikle Amerika Birleşik Devletleri'nde inşa edilmiş köprüleri temsil eden, dört açıklıklı kıstas bir köprü seçilmiştir. Bu kıstas köprüye ait sonlu eleman modeli oluşturulmuş ve bu model kullanılarak, kiriş mesnetlerindeki hareketli yük tesirlerinin dağılımı ile değeri üzerinde, dolayısıyla çekiç başlı köprü ayaklarındaki iç kuvvetler üzerinde, etkileri olan köprü parametrelerini belirlemek maksadıyla duyarlılık analizleri yapılmıştır. Duyarlılık analizleri, kirişler arası mesafenin, kiriş sayısının, kiriş tipinin, döşeme kalınlığının ve döşeme konsolu mesafesinin hareketli yük dağılımı ile değeri üzerinde, dolayısıyla çekiç başlı köprü ayaklarındaki iç kuvvetler üzerinde, kayda değer etkisi olduğunu ortaya çıkarmıştır. Bu doğrultuda, duyarlılık analizlerinin sonuçlarından yola çıkarak her bir parametreye geniş bir aralıkta değer verilerek parametrik analizler yapılmıştır. Elde edilen 50000'den fazla veri üzerinde, en küçük kareler yöntemi kullanılarak başlık kirişinde oluşan maksimum moment ve kesme kuvvetleri, kolonlarda oluşan maksimum moment ile eşlik eden eksenel yük ve maksimum eksenel yük ile eşlik eden momentlerin hesaplanabilmesi için tasarım denklemleri elde edilmiştir. Bu denklemler ile hesaplanan çekiç başlı köprü ayağı

kuvvetlerinin, üç boyutlu sonlu eleman analizleri ile elde edilen sonuçlarla uyumlu olduğu gösterilmiştir.

Anahtar Kelimeler: Çekiç başlı köprü ayakları, hareketli yük dağılımı, tasarım, sonlu eleman modeli

To my family.

ACKNOWLEDGEMENTS

First and foremost, I am deeply grateful for the continuous support, insight and patience of my supervisor, Prof. Dr. Murat Dicleli. Without his constant trust and guidance, I would not be able to complete this thesis. I have learnt so much from him and he was always there to steer me in the right direction, whenever I needed.

Also, I would like to thank to my family. They have always believed in me and supported me every way they could. I dedicated this thesis to them.

TABLE OF CONTENTS

ABSTRACT v

ÖZ vii

ACKNOWLEDGEMENTS x

TABLE OF CONTENTS xi

LIST OF TABLES xiv

LIST OF FIGURES xvi

CHAPTERS

1. INTRODUCTION 1

1.1. Introduction 1

1.2. Research Objective, Scope and Outline 4

1.3. The Benchmark Bridge 6

1.4. Parameters Considered in the Analyses 7

2. DESCRIPTION OF AASHTO - LRFD LIVE LOAD AND 2D MOVING LOAD ANALYSES 9

2.1. Description of AASHTO – LRFD Live Load 9

2.2. 2D Moving Load Analyses 11

3. 3D STRUCTURAL MODEL 15

3.1. Superstructure Modeling 15

3.2. Substructure Modelling 19

4. SENSITIVITY ANALYSES 21

4.1. General 21

4.2. Sensitivity Analysis for the Piers 22

4.3. Sensitivity Analysis for the Girder Spacing 23
4.4. Sensitivity Analysis for the Girder Type 24
4.5. Sensitivity Analysis for the Number of Girders 26
4.6. Sensitivity Analysis for the Number of Spans 27
4.7. Sensitivity Analysis for the Overhang Distance 28
4.8. Sensitivity Analysis for the Slab Thickness 28
4.9. Sensitivity Analysis for the Span Length 29
4.10. Summary of Sensitivity Analyses Results 30
5. DESCRIPTION OF PARAMETRIC ANALYSES AND FORMULATION OF THE DESIGN EQUATIONS 31
5.1. Description of Parametric Analyses 31
5.2. Formulation of the Design Equations 33
5.2.1. Design Equations for the Cap Beam 34
5.2.1.1. Calculation of the Cap Beam Internal Forces via the Principles of Statics 34
5.2.1.2. Regression Analysis Procedure to Formulate the Girder Live Load Reaction Forces 36
5.2.1.3. Equations to Calculate the Maximum Cap Beam Moment and Accompanying Shear Force 38
5.2.1.4. Equations to Calculate the Maximum Cap Beam Shear Force and Accompanying Moment 40
5.2.2. Design Equations for Pier Column and Foundation Design 41
5.2.2.1. Equations to Calculate the Maximum Column Axial Load and Accompanying Moment 41

5.2.2.2. Equations to Calculate the Maximum Column Moment and Accompanying Axial Load 42
6. VERIFICATION OF THE PROPOSED DESIGN EQUATIONS.....43
6.1. Verification via Using the Entire Pool of Data 43
6.2. Verification via Realistic Case Studies of Bridges 51
7. CONCLUSIONS 53
REFERENCES.....57

LIST OF TABLES

TABLES

Table 1.1. Benchmark bridge parameters 7
Table 1.2. Bridge parameters considered in the analyses and their application range 8
Table 2.1. The maximum pier reactions and corresponding live load positions - R (kN) / x (m) 12
Table 3.1. Comparison of sectional properties of idealized section and the actual AASHTO Type III girder section 17
Table 3.2. The maximum girder reactions over the piers (kN) 18
Table 4.1. Sensitivity Analyses Sets 22
Table 4.2 The ratios of the maximum and minimum girder reaction forces to the total reaction force over the pier using a FEM with and without the piers 23
Table 4.3. The ratios of the maximum girder reaction forces to the total reaction force over Pier-1 for various girder spacings 24
Table 4.4. The distribution of the ratios of the girder reaction forces to the total reaction force among the girders over Pier-1 for various girder spacings and single lane loading 24
Table 4.5. Dimensions of the AASHTO girder types 26
Table 4.6. The ratios of the maximum girder reaction forces to the total reaction force over Pier-1 for various girder types 26
Table 4.7. The ratios of the maximum girder reaction forces to the total reaction force over Pier-1 for various number of girders 27
Table 4.8. The ratios of the maximum girder reaction forces to the total reaction force over Pier-1 for various number of spans 27
Table 4.9. The ratios of the maximum girder reaction forces to the total reaction force over Pier–1 for various overhang distances 28

Table 4.10. The ratios of the maximum girder reaction forces to the total reaction force over Pier-1 for various slab thicknesses.....29
Table 4.11. The ratios of the maximum girder reaction forces to the total reaction force over Pier-1 for various span lengths.....30
Table 5.1. Analysis sets considered in parametric analyses.....33
Table 5.2. Coefficients for Eq. 10 to calculate the maximum column face moments, n_c: number of girders resting on the cantilever part of the beam 40
Table 5.3. Coefficients for Eq. 12 to calculate the maximum column face shear forces, Nc: number of girders resting on the cantilever part of the beam.....41
Table 6.1. The average ratio and standard deviation 44
Table 6.2. Test bridge model parameters (w_c = column width in meters) 51
Table 6.3. Comparison of FEM analysis results with design equations results.....51

LIST OF FIGURES

FIGURES

Figure 1.1. Hammer-head Pier Cap 3
Figure 1.2. Details of the benchmark bridge (a) Elevation view, (b) Deck cross-section (all dimensions are in meters) 7
Figure 2.1. (a) HL-93 Design Truck, (b) Two trailing HL-93 trucks, loaded on bridge piers to produce extreme reactions 10
Figure 2.2. Transverse loading of bridge superstructure (dimensions are in meters) 11
Figure 2.3. 2D Structural Model and trailing trucks used for moving load analyses 12
Figure 3.1. Finite element model of superstructure proposed by Hays et. al. (1986) 15
Figure 3.2. 3D finite element model of a two-span bridge 16
Figure 3.3. (a) Idealized Section Compared to AASHTO Girder Type III (dimensions are given in millimeters) (b) Refined FEM for verification purpose 18
Figure 3.4. Substructure modeling 19
Figure 4.1. AASHTO girder types 25
Figure 5.1. Girder live load reaction forces on a typical hammer-head pier 34
Figure 5.2. *Fi vs (a) number of girders, (b) girder spacing, (c),* d_h/S *(d),* K_g*, (e) slab thickness, (f)* d_e 38
Figure 6.1. Comparison of FEM results and proposed equation for $M_{B\text{-}Max}$ / R_{2D} as a function of various parameters (Number of girders = 6, AASHTO Type III girder, S = 2.4 m, d_e = 1.2 m, column width = 2.0 m, t_s = 0.20 m) 46
Figure 6.2. **.** Comparison of FEM results and proposed equation for $V_{B\text{-}Max}$ / R_{2D} as a function of various parameters (Number of girders = 6, AASHTO Type III girder, S = 2.4 m, d_e = 1.2 m, column width = 2.0 m, t_s = 0.20 m) 47
Figure 6.3. *Comparison of FEM results and proposed equation for* $M_{c\text{-}Max}$ / R_{2D} *as a function of various parameters (Number of girders = 6, AASHTO Type III girder, S = 2.4 m,* d_e *= 1.2 m, column width = 2.0 m,* t_s *= 0.20 m)* 48

Figure 6.4. Comparison of FEM results and proposed equation for N_c / R_{2D} as a function of various parameters (Number of girders = 6, AASHTO Type III girder, S = 2.4 m, d_e = 1.2 m, column width = 2.0 m, t_s = 0.20 m) 49
Figure 6.5. Comparison of FEM results and proposed equation for M_c / R_{2D} as a function of various parameters (Number of girders = 6, AASHTO Type III girder, S = 2.4 m, de = 1.2 m, column width = 2.0 m, ts = 0.20 m) 50

CHAPTER 1

INTRODUCTION

1.1. Introduction

Live Load Distribution Factors (LLDFs) are widely used to determine the moment and shear in bridge superstructure components, such as composite prestressed concrete girders. The maximum moment and shear in bridge girders are estimated by first calculating these responses in a 2D beam model under a single design truck. Then, the calculated responses are multiplied by the corresponding LLDFs to get the maximum live load moment or shear in a girder. AASHTO LRFD Bridge Design Specifications (2017) proposes several LLDFs to calculate the moment and shear for exterior and interior girders of bridges with various superstructure configurations. These LLDF formulae are given as a function of girder spacing (S), span length (L), slab thickness (t_s) and longitudinal stiffness factor (K_g), which is a function of the elastic moduli of the superstructure materials, girder section properties and slab thickness.

However, such a simplified procedure to estimate live load effects in bridge substructure components is not available in design codes. For instance, AASHTO (2017) does not propose an approach for determining live load effects in bridge piers. The Federal Highway Administration (FHWA) acknowledges this problem in the manual titled, "Comprehensive Design Example for Prestressed Concrete (PSC) Girder Superstructure Bridge with Commentary" (2003). In the FHWA manual it is stated that accurately determining the maximum live load effects in bridge piers requires a thorough 3D Finite element model (FEM) of the bridge. Using the 3D FEM moving load analysis on the bridge must be carried out and every possible live load location with every possible design lane combination must be checked to find the maximum effects in bridge piers.

Nevertheless, in the aforementioned FHWA (2003) manual, an approach is still proposed for designing piers under live load effects. According to this design approach, first the support reactions at the pier due to the AASHTO HL-93 truck and lane load are calculated using a continuous 2D single beam model of the bridge. The support reaction due to the truck load is then represented by two forces transversely spaced at 1.83 m and the reaction due to the lane load is represented by a uniformly distributed load over a length of 3.3 m. These representative reaction forces are then applied to the deck at the pier location and the load is distributed to the girders assuming that the deck acts as a series of simple spans supported on the girders. While applying the representative live load, the design lane is assumed to be 3.6 m wide and the load is allowed to be moved within the design lane across the bridge width, but not closer than 0.6 m to the edge of the lane. Next, the calculated girder reactions are applied to the pier. The procedure is repeated for one, two, three lanes and so on, considering the multiple presence factors in AASHTO (2017). The maximum effects obtained from all these cases are used as design forces for the pier components. The analysis procedure defined above is quite tedious and yields only a rough estimation of the actual responses under live load.

Another approach employed by bridge engineers to design piers is using the readily available LLDFs for girder design. In this approach, the maximum shear in the girders are calculated using the available LLDFs in AASHTO (2017). Then, the calculated shear is applied to the pier at every girder support location. However, under live load effects, different reaction forces are developed at girder supports depending on the transverse configuration of the live load applied over the lanes. Since LLDFs give the maximum shear force in a girder, using this load at all the supports leads to erroneous results. In fact, a study on the applicability of AASHTO LLDFs to estimate the forces in integral bridge substructures revealed that such equations are not suitable (Erhan & Dicleli, 2009a).

Although, several research studies have been conducted on live load distribution in bridge girders (Cai, 2005; Zokaie, 2000; Huo et al. 2005; Yousif & Hindi, 2007; Barr

et al., 2001; Dicleli & Erhan, 2009) and integral bridge abutments (Erhan & Dicleli, 2009b), research studies to estimate live load effects in bridge piers are scarce in the literature. A study by Williams and Hoit (2004) shows that neural networks can be used for bridge pier design under live load. This study reveals that neural network approach can be easily implemented in design software packages. However, the research is conducted by employing only a limited number of bridges as input for the neural network and no definitive conclusions or design methods are proposed. Accordingly, more practical and accurate design tools are urgently needed to estimate live load effects in bridge piers.

There are several types of bridge piers, such as wall piers, single column piers, multiple column piers and hammer-head piers. Among all these pier types, hammer-head piers (Figure 1.1.) are used most commonly especially in urban areas since cap beams of such piers allow more space under the bridge and they are aesthetically preferable compared to other types of piers (Liu et al., 2015). To design the hammer-head piers, the live load responses in the cap beam and column must be determined. Accordingly, in this research study, design equations are developed to estimate the internal forces in hammer-head bridge piers under live load effects.

Figure 1.1. Hammer-head Pier Cap

1.2. Research Objective, Scope and Outline

The main objective of this research study is to develop reliable and easy-to-use design equations to estimate the live load effects in hammer-head bridge pier components. It is important to emphasize that this study does not target an accurate prediction of the live load responses as recorded on a real bridge in the field. It rather aims at providing an alternative to complicated finite element modeling and analysis of bridges throughout the design process.

The scope of this research study is limited to symmetrical and unskewed continuous slab-on-prestressed-concrete-girder bridges with maximum nine girders supported by hammer-head piers (bridges with more than nine girders becomes quite wide and generally not used in practice). Prestressed concrete girders are used for up to 40 meters of clear span length (Lounis & Cohn, 1993). Accordingly, in this research study, bridges having a span length up to 45 meters (measured between centerlines of supports) are considered.

Design equations to determine live load effects in hammer-head bridge piers are developed following the steps below;

i- First, the FHWA bridge inventory database is inspected to determine a representative span length and number of spans of continuous prestressed concrete girder bridges in the US. Accordingly, a four span symmetrical bridge with a span length of 25 meters is considered as a benchmark bridge for sensitivity analyses to determine the effect of various parameters on live load forces in hammer-head bridge piers.

ii- Then a 2D beam model of the benchmark bridge is built and moving load analyses are performed to determine the longitudinal position of the AASHTO HL-93 live load yielding the maximum reaction at the piers. In addition, similar analyses are performed for continuous bridges with span lengths ranging between 15 and 45 meters where the results are used in sensitivity

analyses to determine the effect of span length on the variation of live load forces in hammer-head bridge piers.

iii- Next, 3D FEMs of the benchmark bridge and those with span lengths ranging between 15 and 45 meters are built and sensitivity analyses are conducted under AASHTO HL-93 live load longitudinally positioned according to the 2D analyses results to determine the effect of various bridge parameters on the variation of live load forces in hammer-head bridge piers. This is achieved by inspecting the variation of the reaction forces at the girder supports across the width of the bridge for the single or multiple truck positions in the transverse direction where the trucks are positioned towards the edge of the deck. In the analyses, the ASSHTO multiple presence factors are considered, where the HL-93 live load is multiplied by a factor, to consider the lower probability of having more than one truck positioned side-by-side across the width of the bridge.

iv- The sensitivity analyses results revealed the bridge parameters that have significant effect on the magnitude and distribution of the live load reactions at the girder supports and hence, the forces in the hammer-head pier. Bridge parameters that do not significantly affect the magnitude and distribution of girder live load reactions are not included in the parametric analyses whose results are used in the formulation of the design equations to determine the live load effects in hammer-head bridge piers.

v- The 3D FEMs of various bridges consisting of a range of bridge parameters that affect the live load distribution in hammer-head bridge piers are constructed. The 3D FEMs are created with every possible combination of bridge parameter to cover a broad range of bridge configuration scenarios. The AASHTO HL-93 live load is then applied at the longitudinal positions along the bridge that were determined via 2D moving load analyses. Transversely,

the AASHTO HL-93 live load is applied on the bridge so that every possible scenario of single or multiple lane loading positions are generated.

vi- Next, support reactions of girders on hammer-head piers are determined for every possible scenario of traverse loading scheme. Subsequently, the transverse loading schemes and associated girder support reactions and their distribution that result in the maximum responses in the hammer-head pier components are determined. This is done for every bridge model in each analysis set.

vii- Then, a minimum least square regression analysis procedure is applied to the generated data in succession for every inspected bridge parameter to obtain design equations for calculating the maximum responses in the hammer-head pier components.

viii- Finally, to verify the proposed design equations, the maximum responses in the hammer-head pier components obtained from the proposed design equations are compared with those obtained from 3D FEM analyses and a reasonably good agreement is found between the two. To further verify the proposed design equations, 3D FEMs of two distinct bridges are built and analyzed under AASHTO HL-93 live load and the internal forces in the hammer-head pier components are determined. Then, the internal forces obtained from the 3D FEM analyses are compared with those from the proposed design equations and a close agreement is found between the two.

1.3. The Benchmark Bridge

The benchmark bridge considered in this study is a four span continuous slab-on-prestressed concrete girder bridge with equal spans of 25 m as shown in Figure 1.2. The properties of the bridge are given in Table 1.1. The deck width and the span length are chosen to be close to the average values obtained from the FHWA inventory for prestressed concrete bridges. The continuity of the spans adjacent to the support affects the magnitude of the live load support reaction. Therefore, the number of spans

is selected as four to have a bridge where both sides of the supports have the cases of exterior-interior and interior-interior spans.

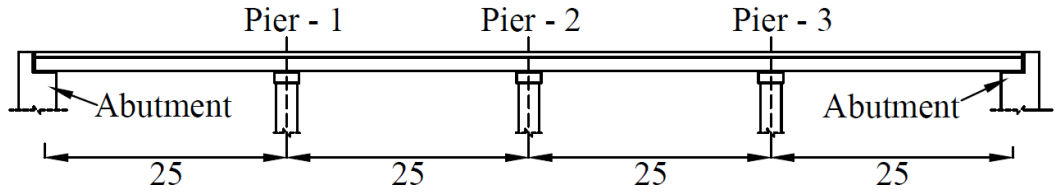

(a)

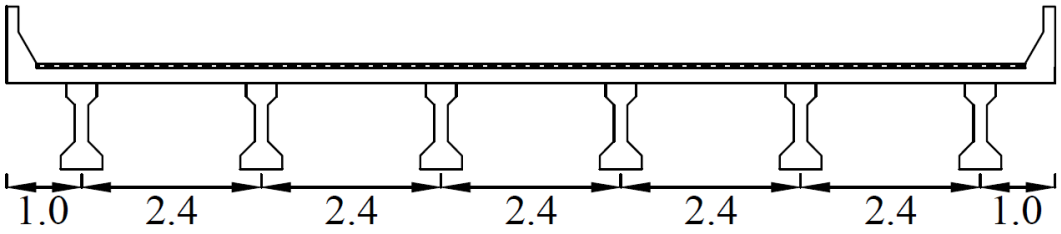

(b)

Figure 1.2. Details of the benchmark bridge (a) Elevation view, (b) Deck cross-section (all dimensions are in meters)

Table 1.1. *Benchmark bridge parameters*

Number of spans (N)	4
Number of girders (N_g)	6
Girder spacing (S)	2.4 m
Span length (L)	25 m
Girder Type	AASHTO Type III Girder
Slab thickness (t_s)	0.20 m
Overhang distance (d_e)	1 m

1.4. Parameters Considered in the Analyses

The bridge parameters considered in this study and their range of variation are given in Table 1.2. Sensitivity analyses are conducted to determine the parameters that affect the live load forces in the components of hammer-head bridge piers. These parameters are then used to develop design equations to estimate the live load effects in hammer-head pier components.

Table 1.2. *Bridge parameters considered in the analyses and their application range*

Number of Spans	2, 3, 4
Span Length (L)	10 - 45 meters
Number of Girders (n)	3 - 9 girders
Girder Spacing (S)	1.2 - 4.8 meters
Girder Type	AASHTO Girder Types I - VI
Slab Thickness (t_s)	0.15 - 0.30 meter
Overhang Distance (d_h)	0 - 2.4 meters
Pier Column Width (w_c)	0.5 - 20 meters

CHAPTER 2

DESCRIPTION OF AASHTO - LRFD LIVE LOAD AND 2D MOVING LOAD ANALYSES

2.1. Description of AASHTO – LRFD Live Load

The AASHTO (2017) HL-93 live load is composed of a three-axle truck as shown in Figure 2.1. (a) and a 9.3 kN/m uniform loading (lane load) applied continuously or in patches along the bridge and distributed over a 3 m width. The truck load is magnified by a dynamic load allowance factor of 1.33 considering the dynamic interaction between the truck and road surface. Dynamic interaction between the truck and road surface occurs due to discontinuities in the road pavement such as surface cracks and deck joints. The dynamic load allowance factor is not applied to the lane load. In order to obtain the maximum support reactions over the piers, AASHTO (2017) requires that two trailing design trucks with 90% of their weight and with a spacing of 15 m between the front axle of the tailgating truck and the rear axle of the leading truck, combined with 90% of lane load be applied over the bridge. The distance between the 145 kN axles of each truck is taken as 4.3 m. (Figure 2.1. (b)) to maximize the support reactions over the piers. Furthermore, similar to the approach used in the development of AASHTO live load distribution factors for the girders (Patrick et al., 2006), neither the design lane load nor the dynamic allowance factor are considered in the live load analyses for the development of design equations to estimate the maximum forces in the hammer-head pier components. However, as the design equations proposed in this research study are normalized by the live load support reaction calculated using a 2D single beam continuous bridge model, the pier response is already decoupled from the magnitude of live load support reactions over the piers. In the 3D analyses where the trailing trucks are placed side-by-side in the transverse direction, AASHTO (2017) requires the use of multiple presence factors to incorporate the lower probability of

simultaneous multiple lane loading in the analyses. The multiple presence factor assumes the values of 1.2, 1.0, 0.85 and 0.65 for single, two, three and four or more loaded lanes respectively. Accordingly, in 3D FEM analyses of the bridge models conducted as part of this research study, multiple presence factors are used to multiply the truck loads as a function of the number of loaded lanes. Furthermore, in 3D analyses, AASHTO (2017) requires that the truck cannot be closer than 0.60 meter to the adjacent lane. Therefore, when multiple design lanes are loaded, a minimum clearance of 1.2 m is provided between the trucks (Figure 2.2.).

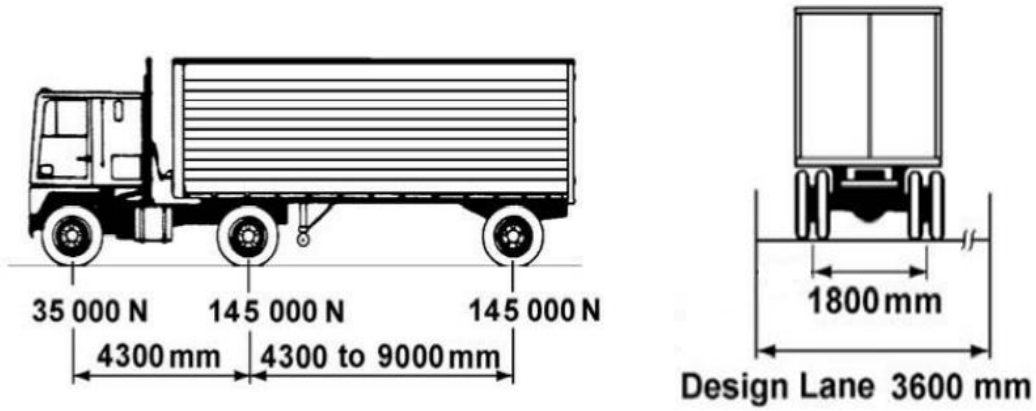

(a)

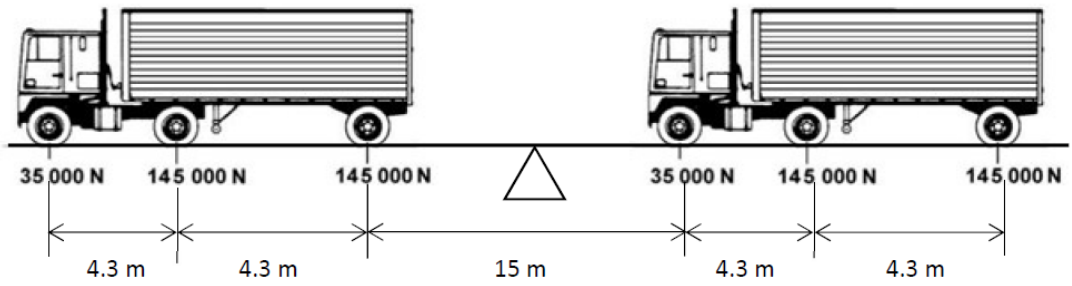

(b)

Figure 2.1. (a) HL-93 Design Truck, (b) Two trailing HL-93 trucks, loaded on bridge piers to produce extreme reactions

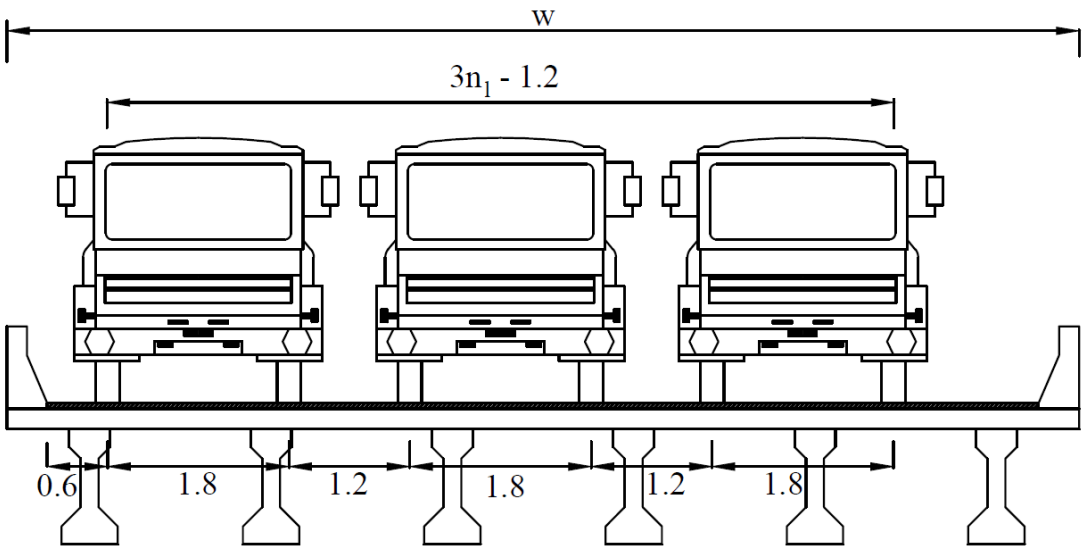

Figure 2.2. Transverse loading of bridge superstructure (dimensions are in meters)

2.2. 2D Moving Load Analyses

2D moving load analyses are conducted to determine the longitudinal positions of the trucks yielding the maximum support reactions at the piers of two, three and four span continuous bridges with equal span lengths of L = 10, 15, 20, 25, 30, 35, 40, 45 meters. For this purpose, 2D beam models of the continuous bridges are built using the finite element software SAP2000 (2009), where roller supports are used at the piers. Then, two AASHTO HL-93 trucks are applied to each bridge model in a trailing configuration (Figure 3.3.) and moved in the longitudinal direction along the bridge to determine the live load positions that create the maximum support reactions over the piers. AASHTO (2017) requires the trailing trucks to be spaced in the longitudinal direction such that the distance between the front axle of the tailgating truck and the rear axle of the leading truck is 15 m. The live load analyses results are presented in Table 2.1. For each one of the cases listed in the table, x is defined as the distance from the leftmost support (abutment) to the front axle of the leading truck as shown in Figure 2.3. For span lengths of 10 and 15 meters, it is not possible to fit all the axles of the two trailing trucks within the spans that are adjacent to the pier. However, the

axles, which do not fall within the spans adjacent to the pier, do not contribute to the maximum reaction and their effects are ignored per AASHTO (2017). The longitudinal positions of the trucks determined via 2D single beam bridge model analyses are used to place the trucks along the bridge in the 3D FEM analyses.

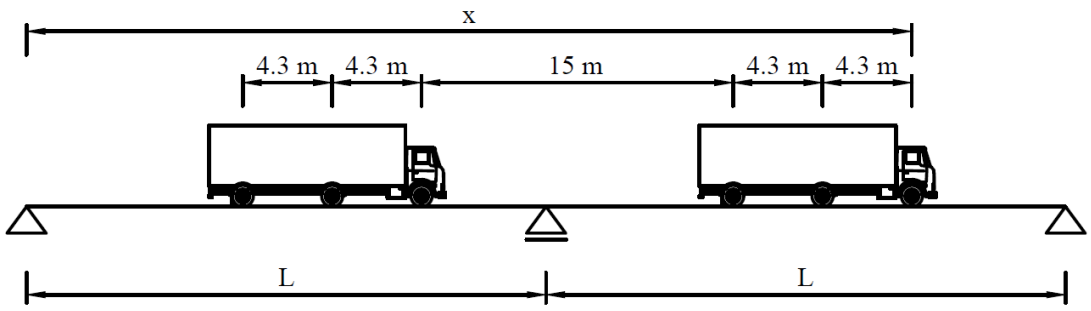

Figure 2.3. 2D Structural Model and trailing trucks used for moving load analyses

Table 2.1. *The maximum pier reactions and corresponding live load positions - R (kN) / x (m)*

Span Length, L (m)	2 Spans	3 Spans		4 Spans		
	Pier - 1	Pier - 1	Pier - 2	Pier - 1	Pier - 2	Pier - 3
10	290 / 15.80	287 / 15.20	286 / 26.50	287 / 15.20	280 / 25.90	286 / 36.50
15	309 / 20.80	308 / 19.90	308 / 36.80	308 / 19.80	303 / 35.80	308 / 51.80
20	332 / 37.60	316 / 25.00	316 / 47.00	316 / 25.00	312 / 45.80	316 / 67.10
25	414 / 42.60	395 / 41.50	395 / 68.60	394 / 41.40	372 / 67.60	394 / 93.70
30	462 / 47.60	448 / 45.80	448 / 79.30	447 / 45.70	427 / 77.60	447 / 109.40
35	493 / 52.60	482 / 50.30	482 / 89.80	481 / 50.20	464 / 87.60	481 / 124.90
40	513 / 57.60	505 / 55.00	505 / 100.20	504 / 54.80	490 / 97.60	504 / 140.30
45	527 / 62.60	52 / 59.60	521 / 110.50	521 / 59.40	508 / 107.60	521 / 155.70

It is noteworthy that in continuous beams, the magnitude and distribution of support reactions are affected by the relative stiffness, EI of the beams in each span (E = modulus of elasticity, I = moment of inertia of the beam). For the continuous bridges under consideration, the girder sizes are identical in all the spans and hence the relative stiffness is always equal to unity. Therefore, the calculated support reactions and associated truck positions are independent of the girder size. This is also proven by conducting moving load analyses using different girder sizes where identical support reactions are obtained.

CHAPTER 3

3D STRUCTURAL MODEL

3.1. Superstructure Modeling

The 3D finite element models (FEMs) of the bridges considered in this study are built using the software SAP2000 (2009).

Four different modeling approaches for slab-on-girder bridge superstructures are compared in the studies conducted by Mabsout et. al (1997) and Yousif and Hindi (2007). Both studies concluded that the model proposed by Hays et al. (1986), although being simple compared to the other three modeling approaches, provides acceptable accuracy. In this model, the slab is idealized by quadrilateral shell elements and the girders are modeled using space frame elements where the center of gravities of slab and girders coincide (Figure 3.1.).

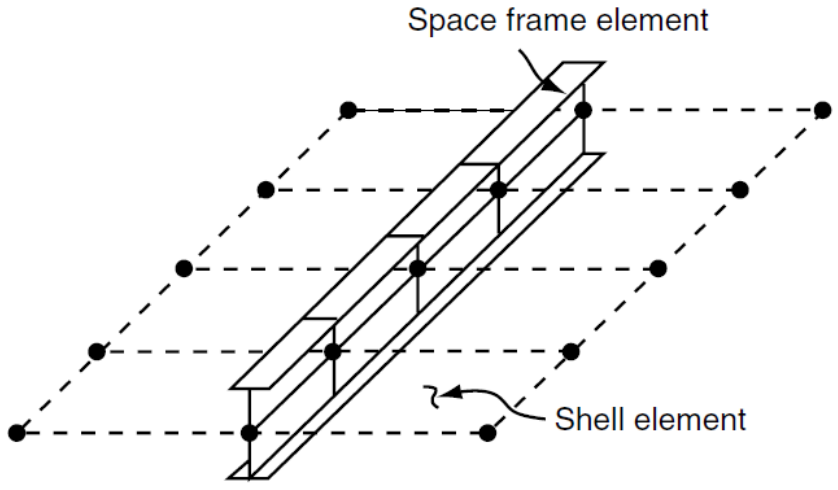

Figure 3.1. Finite element model of superstructure proposed by Hays et. al. (1986)

In this research study, a FEM based on the modeling approach of Hays et al. (1986) is used as shown in Figure 3.2. To facilitate the application of HL-93 live load, shell elements having a width of 0.6 m are used transversely. In the longitudinal direction, the shell elements have a length of 0.5 m. Thus, 0.6 x 0.5 m quadrilateral shell elements are formed for the modeling of the slab. The aspect ratio of the shell elements, which is equal to 0.6/0.5 = 1.2, is below the AASHTO (2017) maximum suggested value of 5.0. The girders are divided into 0.5 m lengths connected between the nodes of the shell elements.

In order to incorporate the composite action between the slab and the girders in the FEM, the moment of inertia of the girders (I_g) in the model is calculated as the moment of inertia of the composite section (I_c), which is composed of the slab and girder, minus the moment of inertia of the slab (I_s) with an assigned tributary width for each girder (Dicleli & Erhan, 2009).

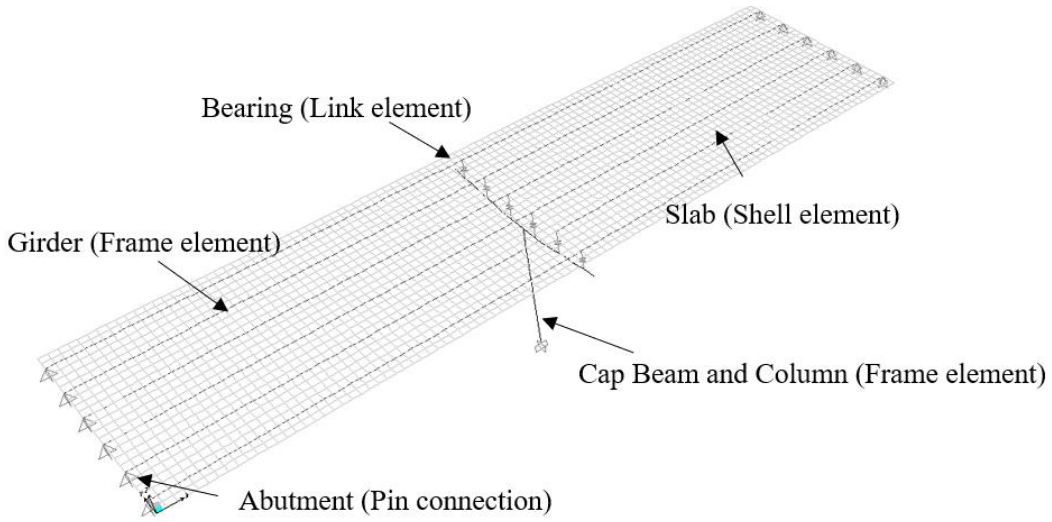

Figure 3.2. 3D finite element model of a two-span bridge

Although, this approach is proven to be accurate, further verification is also made. For this purpose, first, as the top and bottom flanges of the precast girders have variable widths along the flange thickness, simplified rectangular sections representing the original areas of the top and bottom flanges are used such that the depths of the

idealized flanges are chosen to yield the same flange cross-sectional area of the original section (Figure 3.3.(a)). Sectional properties of the idealized girder section are given in Table 3.1., along with the sectional properties of AASHTO Girder Type III for comparison purposes. The data listed in the table shows that the idealized section is a reasonably good approximation of the actual AASHTO Type III Girder. Then, 3D FEM of the benchmark bridge is built by following the approach proposed by Hays et al. (1986) and a more refined modeling approach where the top and bottom flanges as well as the web of the simplified precast girders are modeled using quadrilateral shell elements and the centroid of the top flange is connected to that of the slab with rigid links spaced at 0.5 m (Figure 3.3.(b)). The FEMs are then analyzed under the AASHTO HL-93 live load applied over one, two, three and four design lanes. The maximum girder reactions over the piers are reported in Table 3.2. The analyses results show that the model proposed by Hays et al. (1986), although simple, gives results comparable to those of the more refined model.

Table 3.1. *Comparison of sectional properties of idealized section and the actual AASHTO Type III girder section*

Sectional Properties	AASHTO Beam Type III	Idealized Section	Difference (%)
Cross-Sectional Area (mm^2)	361238	376899	4.34
Moment of Inertia - X Axis (mm^4)	52191212767	52781431690	1.13

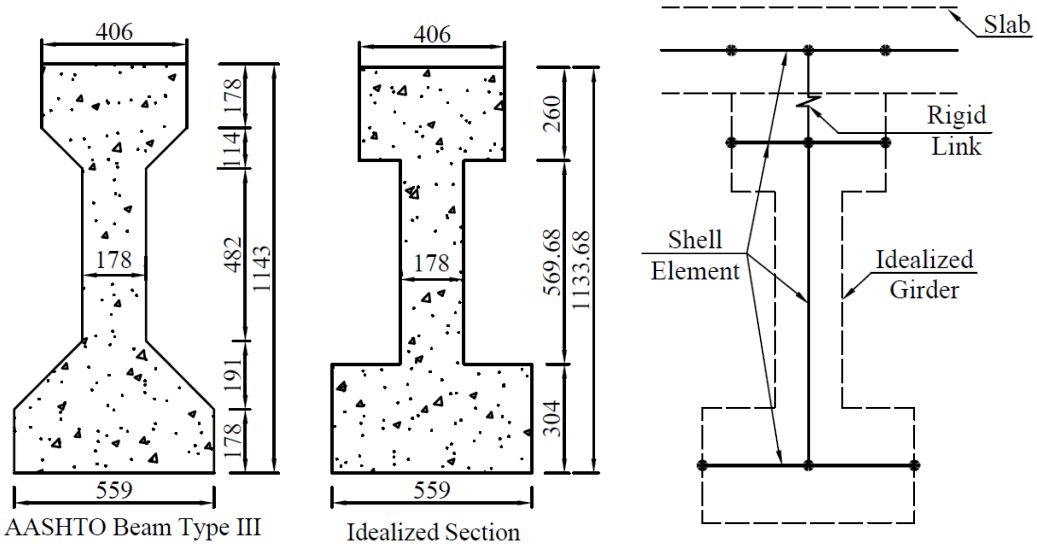

Figure 3.3. (a) Idealized Section Compared to AASHTO Girder Type III (dimensions are given in millimeters) (b) Refined FEM for verification purpose

Table 3.2. *The maximum girder reactions over the piers (kN)*

Number of Design Lanes	Maximum Reaction	FEM of Hays et al. (1986)	More Refined FEM	Difference (%)
1	Pier 1	271.77	262.73	3.44
	Pier 2	257.73	267.79	3.76
	Pier 3	271.58	261.58	3.82
2	Pier 1	250.08	252.36	0.90
	Pier 2	235.31	242.81	3.09
	Pier 3	250.08	253.04	1.17
3	Pier 1	230.73	221.75	4.05
	Pier 2	217.85	214.47	1.58
	Pier 3	230.67	221.81	3.99
4	Pier 1	191.86	190.54	0.69
	Pier 2	181.33	184.00	1.45
	Pier 3	191.75	190.47	0.67

3.2. Substructure Modelling

In the modeling of the hammer-head piers, the cap beam and the column are idealized using 3D beam elements. In the model, the beam elements pass through the centroid of the member cross-sections. The rigidity of the beam-column joint is idealized by using rigid beam members within the joint. The elastomeric bearings between the girders and the cap beam are idealized using link elements with properties equal to those of the bearings. Pin supports are assumed at the abutments and column - foundation connections are assumed to be fixed.

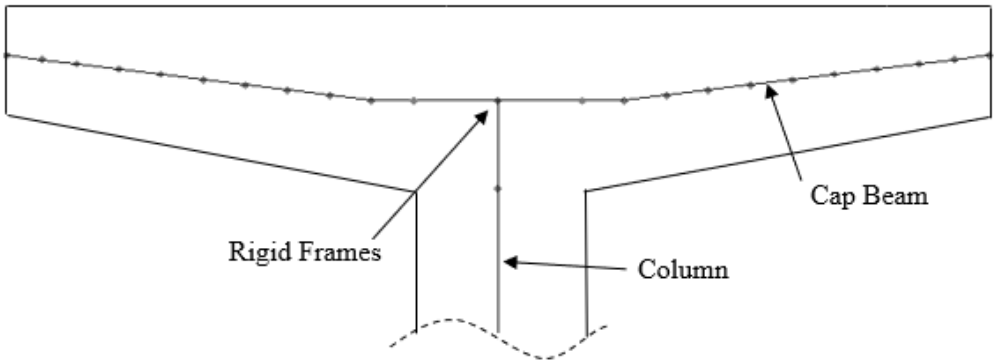

Figure 3.4. Substructure modeling

CHAPTER 4

SENSITIVITY ANALYSES

4.1. General

To identify the bridge parameters that have significant effect on the magnitude and distribution of live load girder reaction forces over the piers and hence, the forces in the hammer-head pier components, sensitivity analyses are conducted. The analyses are conducted by varying the properties of the benchmark bridge as tabulated in Table 4.1. The data presented in bold letters indicates the range of the parameter under consideration for the particular analysis case. For this purpose, first, the 3D FEM of the benchmark bridge is constructed. Then, for each sensitivity analysis case presented in Table 4.1., different 3D structural FEMs are built with varying values of the bridge property that is under consideration, while keeping all the other parameters constant. Every bridge model is analyzed under the AASHTO HL-93 live load applied over one, two, three and four design lanes. The analyses results are presented as the ratio of the girder reaction force to the total support reaction over the pier to enable a comparable presentation of the reaction forces for various analyses cases. Next, the magnitude and distribution of the girder reaction force ratios over the piers is inspected for each parameter and a decision is made whether the bridge parameter under consideration is a significant parameter or not. A separate sensitivity analysis is conducted to assess the need to include the piers in the FEM.

Table 4.1. *Sensitivity Analyses Sets*

Sensitivity Analysis Set	Girder Spacing (m)	Girder Type	Number of Girders	Number of Spans	Overhang Distance (m)	Slab Thickness (m)	Span Length (m)
1	**1.2, 1.5, 1.8, 2.1, 2.4, 2.7**	AASHTO Type III	6	4	1	0.2	25
2	2.4	**AASHTO Type I, II, III, IV, V, VI**	6	4	1	0.2	25
3	2.4	AASHTO Type III	**3, 4, 5, 6, 7, 8, 9**	4	1	0.2	25
4	2.4	AASHTO Type III	6	**2, 3, 4**	1	0.2	25
5	2.4	AASHTO Type III	6	4	**0, 0.50, 1.00, 1.50, 2.00**	0.2	25
6	2.4	AASHTO Type III	6	4	1	**0.15, 0.20, 0.22, 0.25, 0.30**	25
7	2.4	AASHTO Type III	6	4	1	0.2	**10, 15, 20, 25, 30, 35, 40, 45**

4.2. Sensitivity Analysis for the Piers

To assess the need to include the piers in the FEM, analyses of the benchmark bridge model is performed by including and then removing the piers from the FEM. In the model without the piers, roller supports are considered under the girders. The analyses are presented in Table 4.2. in terms of the ratio of the maximum and minimum girder reaction forces to the total reaction force over the piers. The analyses results reveal that the substructure has a negligible effect on the magnitude and distribution of girder

reaction forces and hence, the forces in the hammer-head pier components. This is expected as the vertical deformation of the pier under live load is negligible. Based on this finding, the remaining analyses are conducted using a FEM without the piers.

Table 4.2 The ratios of the maximum and minimum girder reaction forces to the total reaction force over the pier using a FEM with and without the piers

Pier	Number of Loaded Lanes	With Substructure		Without Substructure	
		Maximum	Minimum	Maximum	Minimum
1	1	0.58	-0.02	0.59	-0.03
	2	0.32	-0.03	0.32	-0.03
	3	0.23	0.02	0.23	0.01
	4	0.19	0.19	0.19	0.19
2	1	0.58	-0.02	0.59	-0.02
	2	0.32	-0.03	0.32	-0.03
	3	0.23	0.01	0.23	0.01
	4	0.19	0.19	0.19	0.19
3	1	0.58	-0.02	0.59	-0.03
	2	0.32	-0.03	0.32	-0.03
	3	0.23	0.02	0.23	0.01
	4	0.19	0.19	0.19	0.19

4.3. Sensitivity Analysis for the Girder Spacing

To assess the effect of the girder spacing on the magnitude and distribution of the girder reaction forces, sensitivity analyses are conducted by building and analyzing the FEMs of the benchmark bridge with girder spacings of 1.2 m, 1.5 m, 1.8 m, 2.1 m, 2.4 m and 2.7 m under the AASHTO HL-93 live load applied over one, two, three and four design lanes. However, for the cases where the girder spacing is small, it was not possible to apply the live load up to four design lanes. The analyses results, in terms of the ratio of the maximum girder reaction forces to the total reaction force over Pier-1 (Figure 1.2.), are presented in Table 4.3. The results for the other piers are similar and hence are not presented. In addition, the ratios of the girder reaction forces across the width of the bridge to the total support reaction over Pier-1 are presented in Table 4.4. The table shows the distribution of the total reaction force among the girders for

the case of single lane loading. In the following subsections, however, a similar table is not presented, since a difference in the magnitude of the reaction forces for different values of the parameter under consideration also indicates a different pattern of distribution of the total reaction force among the girders. The analyses results reveal that especially for smaller number of loaded design lanes, there is a significant discrepancy in the magnitude and distribution of girder reactions as a function of the girder spacing. This is expected since the truck wheel loads are distributed by the bending rigidity of the slab between the girders and hence one may expect a better distribution of the load as the girder spacing decreases.

Table 4.3. *The ratios of the maximum girder reaction forces to the total reaction force over Pier-1 for various girder spacings*

Number of Loaded Lanes	1.2 m	1.5 m	1.8 m	2.1 m	2.4 m	2.7 m
1	0.45	0.49	0.53	0.56	0.59	0.61
2	0.20	0.24	0.27	0.30	0.32	0.34
3	-	-	0.17	0.20	0.23	0.25
4	-	-	-	-	0.19	0.19

Table 4.4. *The distribution of the ratios of the girder reaction forces to the total reaction force among the girders over Pier-1 for various girder spacings and single lane loading*

Girder	1.2 m	1.5 m	1.8 m	2.1 m	2.4 m	2.7 m
1	0.45	0.49	0.53	0.56	0.59	0.61
2	0.27	0.29	0.30	0.31	0.32	0.32
3	0.20	0.19	0.17	0.15	0.13	0.10
4	0.11	0.08	0.06	0.03	0.01	0.00
5	0.06	0.02	0.00	-0.01	-0.02	-0.02
6	-0.08	-0.07	-0.05	-0.04	-0.03	-0.02

4.4. Sensitivity Analysis for the Girder Type

To assess the effect of the girder type on the magnitude and distribution of the girder reaction forces and hence, the forces in the hammer-head pier components, sensitivity analyses are conducted by building and analyzing the FEMs of the benchmark bridge

with different girder types. For this purpose, 3D FEMs of the benchmark bridge with AASHTO Girder types I, II, III, IV, V and VI are built and analyzed as described above. In Figure 4.1. typical AASHTO girder types are illustrated and in Table 4.5., corresponding dimensions for each AASHTO girder type is presented. The analyses results, which are presented in Table 4.6., reveal that especially for smaller number of loaded design lanes, a discrepancy as much as 8.4% in the maximum girder reaction ratios is observed as a function of the girder type. This is expected as the rigidity of the girder relative to that of the slab affects the distribution of the live load support reactions among the girders.

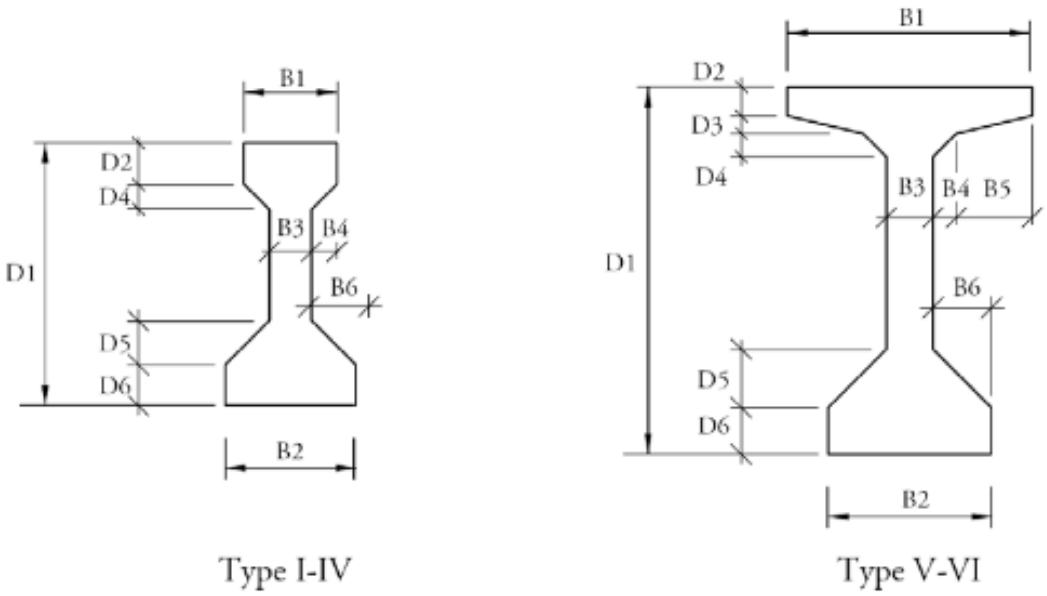

Figure 4.1. AASHTO girder types

Table 4.5. *Dimensions of the AASHTO girder types*

Type	D1	D2	D3	D4	D5	D6	B1	B2	B3	B4	B5	B6
I	71.12	10.16	0	7.62	12.7	12.7	30.48	40.64	15.24	7.62	0	12.7
II	91.44	15.24	0	7.62	15.24	15.24	30.48	45.72	15.24	7.62	0	15.24
III	114.3	17.78	0	11.43	19.05	17.78	40.64	55.88	17.78	11.43	0	19.05
IV	137.16	20.32	0	15.24	22.86	20.32	50.8	66.04	20.32	15.24	0	22.86
V	160.02	12.7	7.62	10.16	25.4	20.32	106.68	71.12	20.32	10.16	33.02	25.4
VI	182.88	12.7	7.62	10.16	25.4	20.32	106.68	71.12	20.32	10.16	33.02	25.4

Table 4.6. *The ratios of the maximum girder reaction forces to the total reaction force over Pier-1 for various girder types*

Number of Loaded Lanes	I	II	III	IV	V	VI
1	0.54	0.56	0.58	0.58	0.59	0.59
2	0.33	0.33	0.32	0.33	0.34	0.34
3	0.23	0.23	0.23	0.23	0.23	0.23
4	0.18	0.18	0.19	0.19	0.19	0.19

4.5. Sensitivity Analysis for the Number of Girders

To assess the effect of the number of girders on the magnitude and distribution of the girder reaction forces, sensitivity analyses are conducted by building and analyzing the FEMs of the benchmark bridge having 3, 4, 5, 6, 7, 8 and 9 girders. However, in the case of larger number of girders, it was possible to apply the AASHTO HL-93 live load for up to six design lanes. The analyses results are presented in Table 4.7. It is observed that the difference between the maximum girder reaction ratios could be as much as 18%. Such a discrepancy is expected since as the number of girders increases the live load is distributed over more girders.

Table 4.7. *The ratios of the maximum girder reaction forces to the total reaction force over Pier-1 for various number of girders*

Number of Loaded Lanes	3 Girders	4 Girders	5 Girders	6 Girders	7 Girders	8 Girders	9 Girders
1	0.61	0.60	0.59	0.59	0.59	0.59	0.59
2	0.39	0.32	0.32	0.32	0.32	0.32	0.32
3	-	-	0.23	0.23	0.23	0.23	0.23
4	-	-	-	0.19	0.17	0.17	0.17
5	-	-	-	-	-	0.14	0.14
6	-	-	-	-	-	-	0.13

4.6. Sensitivity Analysis for the Number of Spans

To assess the effect of the number of spans on the magnitude and distribution of the girder reaction forces, sensitivity analyses are conducted by building and analyzing the FEMs of the benchmark bridge having two, three and four spans. The analyses results presented in Table 4.8. reveal that the number of spans have only a marginal effect on the distribution of the girder reaction forces. The total reaction forces over the piers may be different, however, the distribution of these reaction force among the girders is nearly independent of the number of spans. That is, the girder reaction forces normalized with respect to the total reaction force over the pier is similar for all the piers.

Table 4.8. *The ratios of the maximum girder reaction forces to the total reaction force over Pier-1 for various number of spans*

Number of Loaded Lanes	2 Spans	3 Spans	4 Spans
1	0.57	0.57	0.57
2	0.32	0.32	0.32
3	0.23	0.23	0.23
4	0.19	0.19	0.19

4.7. Sensitivity Analysis for the Overhang Distance

The overhang distance is defined as the distance from the centerline of the exterior girder to the edge of the bridge deck. To assess the effect of the overhang distance on the magnitude and distribution of the girder reaction forces, sensitivity analyses are conducted by building and analyzing the FEMs of the benchmark bridge with overhang distances of 0 m, 0.5 m, 1.00 m, 1.50 m and 2.00 m. The analyses results are presented in Table 4.9. It is observed that there is a significant discrepancy as much as 51% between the maximum girder reaction ratios as a function of the overhang distance. Such a large discrepancy is expected since the overhang part of the slab is a cantilever structure affecting the position of the truck wheel load with respect to the exterior girder, and hence the distribution of the total live load among the girder supports.

Table 4.9. *The ratios of the maximum girder reaction forces to the total reaction force over Pier–1 for various overhang distances*

Number of Loaded Lanes	0 m	0.50 m	1.00 m	1.50 m	2.00 m
1	0.41	0.46	0.59	0.71	0.84
2	0.30	0.31	0.32	0.41	0.51
3	0.23	0.23	0.23	0.26	0.33
4	0.19	0.19	0.19	0.19	0.24

4.8. Sensitivity Analysis for the Slab Thickness

To assess the effect of the slab thickness on the magnitude and distribution of the girder reaction forces, sensitivity analyses are conducted by building and analyzing the FEMs of the benchmark bridge for a range of slab thicknesses. The analyses results, in terms of the ratio of the maximum girder reaction forces to the total reaction force over the piers, are presented in Table 4.10. The analyses results reveal that especially for smaller number of loaded design lanes, there is a discrepancy as much as 10% in the maximum girder reaction ratios as a function of the slab thickness. This

is expected since a better distribution of live load among the girders is anticipated for stiffer slabs.

Table 4.10. *The ratios of the maximum girder reaction forces to the total reaction force over Pier-1 for various slab thicknesses*

Number of Loaded Lanes	0.15 m	0.20 m	0.22 m	0.25 m	0.30 m
1	0.59	0.58	0.57	0.55	0.53
2	0.33	0.32	0.32	0.32	0.32
3	0.23	0.23	0.23	0.23	0.23
4	0.19	0.19	0.19	0.18	0.18

4.9. Sensitivity Analysis for the Span Length

To assess the effect of the span length on the magnitude and distribution of the girder reaction forces and hence, the forces in the hammer-head pier components, sensitivity analyses are conducted by building and analyzing the FEMs of the benchmark bridge with span lengths of 10 m, 15 m, 20 m, 25 m, 30 m, 35 m, 40 m and 45 m. It is noteworthy that the longitudinal positions of the HL-93 truck, which produce the maximum reactions over the piers for each span length was already determined by 2D moving load analyses as described in detail earlier. The analyses results presented in Table 4.11. show that the effect of the span length on the magnitude and distribution of the girder reaction force ratios are negligible. The span length may normally affect the magnitude of the total live load reaction force over the pier. However, the variation in the distribution of this total reaction force among the girder supports for different span lengths is negligible.

Table 4.11. *The ratios of the maximum girder reaction forces to the total reaction force over Pier-1 for various span lengths*

Number of Loaded Lanes	10 m	15 m	20 m	25 m	30 m	35 m	40 m	45 m
1	0.56	0.58	0.58	0.58	0.57	0.56	0.56	0.55
2	0.35	0.35	0.35	0.32	0.32	0.32	0.33	0.33
3	0.24	0.23	0.23	0.23	0.23	0.23	0.23	0.23
4	0.20	0.20	0.19	0.19	0.19	0.19	0.19	0.18

4.10. Summary of Sensitivity Analyses Results

Based on the sensitivity analyses results, the girder spacing, girder type, number of girders, overhang distance and slab thickness are found to affect the magnitude and distribution of the girder reaction forces and hence included as parameters in the development of design equations to estimate live load effects in hammer-head pier components.

CHAPTER 5

DESCRIPTION OF PARAMETRIC ANALYSES AND FORMULATION OF THE DESIGN EQUATIONS

5.1. Description of Parametric Analyses

To develop design equations to estimate the live load effects in hammer-head piers, parametric analyses under AASHTO HL-93 live load are conducted on the bridges considered in this study by varying the properties, which are found to affect the magnitude and distribution of the girder reaction forces and hence, the forces in the hammer-head pier components. Table 5.1. presents the parametric analyses sets and the range of assigned values of the parameters considered in the analyses.

In Analysis Set 1, the girder type is considered as the primary parameter. However, both the number of girders and the overhang distance is varied simultaneously to cover a broad range of possible bridge configurations. Furthermore, as the overhang distance is found to have a significant effect on the magnitude and distribution of the girder reaction forces, its range of variation applicable to the analyses case under consideration (the overhang distance is taken as not larger than 50% of the girder spacing) is included in all the analyses cases. This resulted in a total of 126 FEMs for Analysis Set 1.

In Analysis Set 2, the slab thickness is considered as the primary parameter. However, as the effect of the slab thickness on the magnitude and distribution of the girder reaction forces is found to be influenced by the number of girders and girder spacing, a range of values are also assigned to these parameters in combination with those of the slab thickness. This resulted in a total of 252 FEMs for Analysis Set 2.

In Analysis Set 3, every combination of girder spacing and number of girders is considered so that every potential bridge width and associated number of lanes considered in this study are made available for parametric analyses. This resulted in a total of 483 FEMs for Analysis Set 3.

In the case of Analysis Set 4, every combination of the slab thickness and girder type are considered. This enabled the consideration of all possible values of the sectional properties of the composite superstructure (slab + girders). This resulted in a total of 72 FEMs for Analysis Set 4.

3D FEMs of each bridge with properties specified in Table 5.1., are built using SAP2000 (2009). In total, 933 FEMs are built and analyzed for various longitudinal and transverse configurations of the trucks. This resulted in more than 10000 analyses cases. Then, regression analyses are conducted on the parametric analyses results to formulate the design equations to estimate the live load effects in hammer-head pier components. It is worth noting that in each analysis case, girder reactions for every possible scenario of live loading are calculated. The width of the column in the hammer-head pier is also kept as a variable where the column width is varied between 0.5 m and the width determined by the distance between the exterior girders.

As the span length is found not to affect the ratio of the girder reaction forces to the total support reaction over the pier as well as the distribution of the reaction forces among the girders, the benchmark bridge with four 25 m long equal spans is used in the parametric analyses. The longitudinal position of the AASHTO HL-93 live load was already determined via 2D moving load analyses. For the transverse position of the single or multiple trucks, the AASHTO HL-93 live load is applied on the bridge so that every possible scenario of single or multiple loading positions of the design lanes are generated across the width of the bridge also considering the multiple presence factor for the loading under consideration.

In the case of the cap beam, for each analysis case, the largest moment with accompanying shear and the largest shear with accompanying moment from all the possible scenarios of live loading are calculated and recorded along with the value of each girder reaction force on the cantilever part of the cap beam. These data are then used in the development of the design equations to estimate live load effects in the cap beam.

In the case of the columns and foundations, for each analysis case, the largest moment with associated axial load and the largest axial load with associated moment from all the possible scenarios of live loading are calculated and recorded and then used in the development of the design equations to estimate live load effects in the column and foundation.

Table 5.1. *Analysis sets considered in parametric analyses*

Parametric Analysis Set	AASHTO Girder Type	Slab Thickness (m)	Girder Spacing (m)	Number of Girders	Overhang Distance (m)	Total Number of Analyses
1	I, II, III, IV, V, VI	0.2	2.4	3, 4, 5, 6, 7, 8, 9	0, 0.6, 1.2	126
2	III	0.15, 0.20, 0.25, 0.30	1.2, 2.4, 3.6	3, 4, 5, 6, 7, 8, 9	0, 0.6, 1.2, 1.8	252
3	I, III, VI	0.2	1.2, 1.8, 2.4, 3.0, 3.6, 4.2, 4.8	3, 4, 5, 6, 7, 8, 9	0, 0.6, 1.2, 1.8, 2.4	483
4	I, II, III, IV, V, VI	0.15, 0.20, 0.25, 0.30	2.4	6	0, 0.6, 1.2	72

5.2. Formulation of the Design Equations

As the magnitude of the girder reaction forces relative to the total reaction force over the pier and their distribution are nearly identical for all the piers, Pier-1 (Figure 1.2.) is considered in the development of the design equations to estimate the live load effects in hammer-head pier components. A typical hammer-head pier supporting nine girders and the associated girder live load reactions are illustrated in Figure 5.1. This figure is used as a reference in the following subsections to formulate the design equations to estimate the maximum moment, shear and axial load responses in the hammer-head pier components.

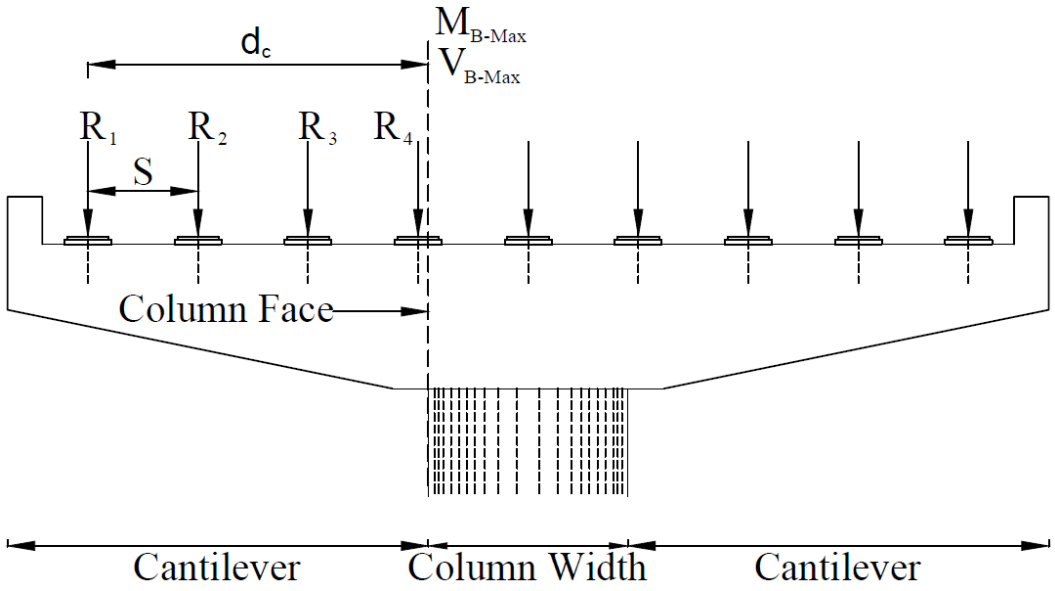

Figure 5.1. Girder live load reaction forces on a typical hammer-head pier

5.2.1. Design Equations for the Cap Beam

5.2.1.1. Calculation of the Cap Beam Internal Forces via the Principles of Statics

In the case of the hammer-head pier cap beam, the live load does not create any axial force (Figure 5.1.). Accordingly, for the design of the cap beam, the maximum moment and the maximum shear with accompanying moment are needed (although it is not considered often in practice, the presence of moment may affect the shear capacity of the reinforced concrete members).

Initially a method based on directly formulating the cap beam responses via regression analyses was tried but was found to yield only rough estimates of the responses obtained from FEM analyses. Accordingly, a method based on the girder live load support reactions was adopted using the principles of statics as explained below to estimate the internal forces in the cap beam.

As observed from Figure 5.1., the girder reactions on the cantilever part of the cap beam of a hammer-head pier create the maximum live load moment and shear at the column face. Accordingly, the maximum live load moment of the cap beam, $M_{B\text{-}Max}$, is calculated by summing up the moments created by each reaction force of the girders

resting on the cantilever part of the cap beam with respect to the column face and expressed in the following form:

$$M_{B-Max} = R_1 d_c + R_2(d_c - S) + R_3(d_c - 2S) + \cdots + R_i(d_c - (i-1)S) + \cdots \quad (1)$$

where $R_1, R_2, R_3 \ldots R_i$ (R_i: the reaction of the ith girder) are the girder reaction forces within the cantilever part of the cap beam, S is the girder spacing and d_c is the distance between the exterior girder and the column face (Figure 5.1.). Alternatively, Eq. 1 may be expressed in an abbreviated form as follows:

$$M_{B-Max} = \sum_i^{n_c} R_i[d_c - (i-1)S] \quad (2)$$

where n_c is the number of girders within the cantilever part of the cap beam and i is the girder number counted starting from the exterior girder (i.e. exterior girder reaction is designated as R_1).

The shear force, V_B at the column face, which accompanies the $M_{B\text{-}Max}$, is calculated via the following equation.

$$V_B = \sum_i^{n_c} R_i \quad (3)$$

Similarly, the maximum shear force, $V_{B\text{-}Max}$, at the column face due to live load is obtained using the equation given below:

$$V_{B-Max} = \sum_i^{n_c} R_i \quad (4)$$

It is noteworthy that $V_{B\text{-}Max}$ may be due to a transverse configuration of the trucks different than that of $M_{B\text{-}Max}$. The moment, M_B, accompanying $V_{B\text{-}Max}$ is calculated using the following equation;

$$M_B = \sum_i^{n_c} R_i[d_c - (i-1)S] \quad (5)$$

Based on the above equations, the girder live load support reactions within the cantilever part of the cap beam need to be determined to calculate the live load responses for the design of the cap beam.

5.2.1.2. Regression Analysis Procedure to Formulate the Girder Live Load Reaction Forces

Minimum least squares regression analyses are performed on the girder live load support reaction data obtained from parametric analyses to develop equations to approximate R_i. The regression analyses are performed considering the parameters obtained from sensitivity analyses. For this purpose, first, the girder reaction data obtained from the parametric analyses are normalized with respect to the pier reaction force obtained from 2D moving load analysis. Then, the normalized data (F) is plotted as a function of one of the parameters. Subsequently, a minimum least square power function is fitted to the plot to obtain an equation in the form given below;

$$F_1 = a_1 \, P_1^{b_1} \tag{6}$$

where, F_1 is the minimum least square regression approximation of the girder live load reaction force under consideration and P_1 is the first parameter that is plotted against F.

Next, the girder live load reaction data is divided by F_1 to decouple the data from the effect of the first parameter P_1. Then, the ensuing data is plotted as a function of the second parameter, P_2 and a minimum least square power function is fitted to the plot to obtain an equation in the following form;

$$F_2 = F/F_1 = a_2 \, P_2^{b_2} \tag{7}$$

This procedure is followed for every parameter under consideration. Consequently, an equation in the following form is obtained:

$$F = a \prod_i^{n_p} P_i^{b_i} \tag{8}$$

where, a is given as:

$$a = \prod_i^{n_p} a_i \tag{9}$$

In the above equation, n_p designates the total number of parameters considered in regression analyses. This procedure is repeated for each reaction force for the cases of one, two, three and four girders on the cantilever part of the cap beam. Consequently, 1+2+3+4 =10 equations are obtained via regression analyses to calculate the support reactions for the cases of one, two, three and four girders on the cantilever part of the cap beam. For instance, considering a bridge with five girders and assuming that there are two girders on the cantilever part of the cap beam, two equations are obtained via regression analyses to calculate the girder reaction forces R_1 and R_2. As an example to the above defined procedure, Figure 5.2. shows the plots of F_i versus the parameters considered in the regression analyses for the case of only one girder on the cantilever part of the cap beam. The curves presented by solid lines show the power function obtained by minimum least squares regression analysis. It is noteworthy that considering the ability of power functions to fit many forms of variations and its simple expression, it is used in the development of the proposed design equations.

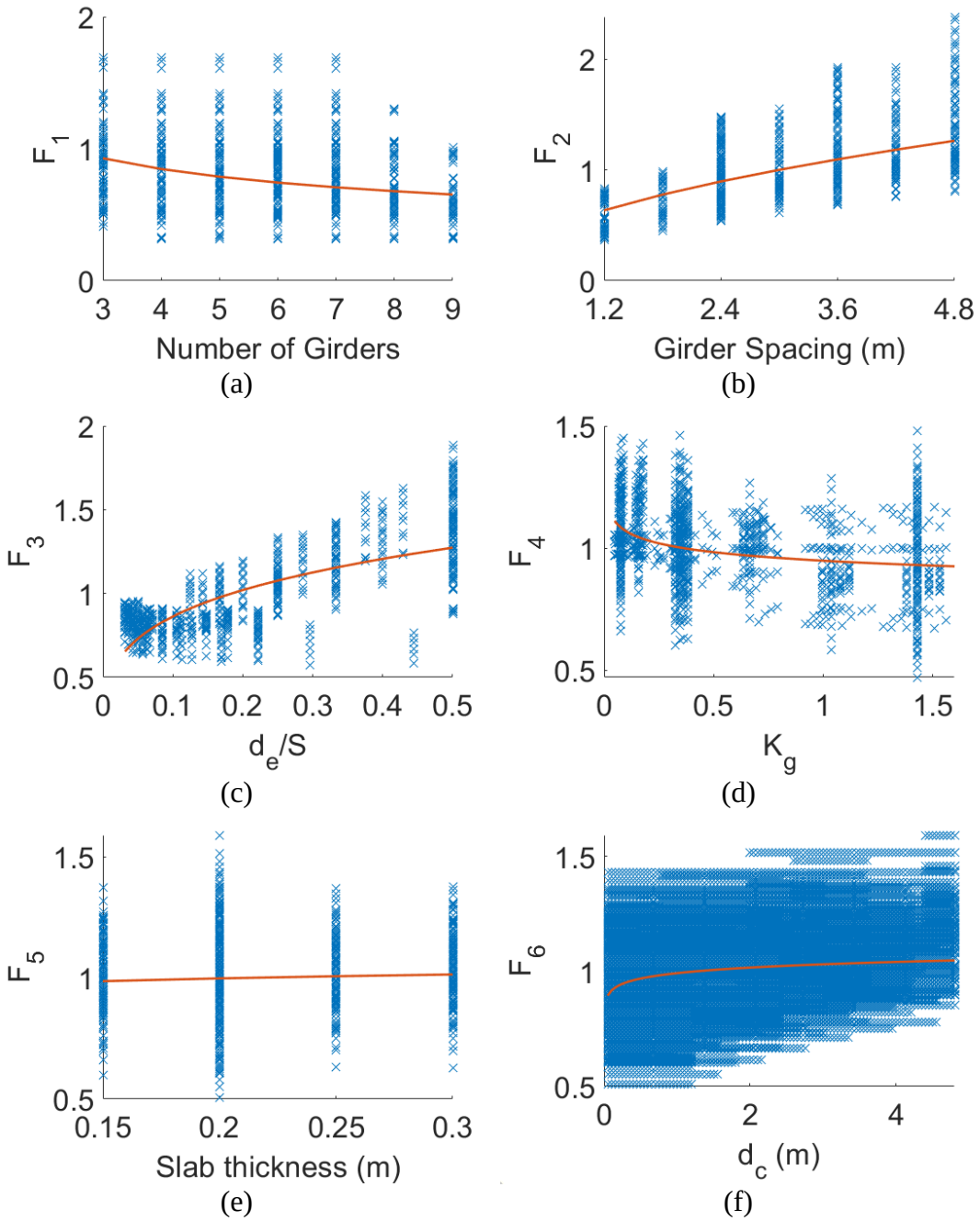

Figure 5.2. *Fi vs (a) number of girders, (b) girder spacing, (c),* d_h/S *(d),* K_g*, (e) slab thickness, (f)* d_e

5.2.1.3. Equations to Calculate the Maximum Cap Beam Moment and Accompanying Shear Force

Following the procedure described in the above section, a set of equations in the form given below are obtained as a function of the parameters considered in the parametric

analyses to calculate the live load support reactions of the girders resting on the cantilever part of the cap beam;

$$R_{M\,i,j} = (a_{i,j}\, N^{b_{1,i,j}}, S^{b_{2,i,j}}\, (d_e/S)^{b_{3,i,j}}\, K_g^{b_{4,i,j}}\, t_s^{b_{5,i,j}} d_c^{b_{6,i,j}}) x R_{2D} \qquad (10)$$

where, $R_{M\,i,j}$ is the reaction force used in the calculation of the maximum cap beam moment and accompanying shear, N is the number of girders, d_e is the overhang distance, t_s is the slab thickness, K_g is the longitudinal stiffness parameter, $a_{i,j}$, $b_{1,i,j}$, $b_{2,i,j}$, $b_{3,i,j}$, $b_{4,i,j}$, $b_{5,i,j}$, $b_{6,i,j}$ are the coefficients to be determined via the minimum least squares regression analyses and R_{2D} is the maximum live load reaction force over the pier as calculated via 2D moving load analyses. The index *i* here designates the girder live load reaction number and the index *j* designates the cases of one, two, three and four girders over the cantilever part of the cap beam. The longitudinal stiffness parameter, K_g is defined as (AASHTO, 2017):

$$K_g = n(I + Ae_g^2) \qquad (11)$$

where, n is the ratio of the modulus of elasticity of the beam material to the modulus of elasticity of the girder material, A and I are respectively the cross-section area and moment of inertia of the girder while e_g is the distance between the centroids of the girder and slab.

It is noteworthy that the distance between the exterior girder and the column face, d_c, is found to have a significant effect on the magnitude of $M_{B\text{-}Max}$. This was realized after formulating Eqs. 1 and 2 and hence, it is included in the minimum least squares regression analyses along with the parameters determined via sensitivity analyses.

The coefficients, $a_{i,j}$, $b_{1,i,j}$, $b_{2,i,j}$, $b_{3,i,j}$, $b_{4,i,j}$, $b_{5,i,j}$, and $b_{6,i,j}$ in Eq. 10 are given in Table 5.2. for the cases of one, two, three and four girders on the cantilever part of the cap beam. These coefficients are substituted in Eq. 10 along with the values of the bridge parameters to calculate the magnitude of the girder live load reaction forces over the cantilever part of the cap beam. These reaction forces are then substituted in Eq. 2 to

calculate the maximum moment and in Eq. 3 to calculate the accompanying shear force in the cap beam.

Table 5.2. *Coefficients for Eq. 10 to calculate the maximum column face moments, n_c: number of girders resting on the cantilever part of the beam*

n_c	i	$a_{i,j}$	$b_{1,i,j}$	$b_{2,i,j}$	$b_{3,i,j}$	$b_{4,i,j}$	$b_{5,i,j}$	$b_{6,i,j}$
1	1	1.2	-0.35	0.5	0.25	-0.05	0.04	0.05
2	1	0.75	-0.2	0.5	0.25	-0.1	0.1	0.15
	2	0.25	0.1	0.8	-0.15	0.04	-0.06	0.06
3	1	0.55	-0.01	0.4	0.3	-0.1	0.15	0.2
	2	0.15	0.35	0.8	-0.03	0.2	-0.25	-0.025
	3	0.4	0.13	-0.1	-0.2	-0.02	0.25	-0.01
4	1	1	-0.25	0.35	0.2	-0.12	0.2	0.1
	2	0.5	-0.12	0.75	-0.03	0.05	-0.1	-0.01
	3	0.06	0.6	0.6	-0.03	0.07	-0.15	0.04
	4	0.0002	3.5	-0.2	-0.03	-0.1	0.7	0.15

5.2.1.4. Equations to Calculate the Maximum Cap Beam Shear Force and Accompanying Moment

Following a procedure similar to that employed in the previous section, the girder live load reaction forces ($R_{V\,i,j}$) to calculate the maximum shear force in the cap beam are formulated as follows;

$$R_{V\,i,j} = (a_{i,j}\, N^{b_{1,i,j}}\, S^{b_{2,i,j}}\, (d_h/S)^{b_{3,i,j}}\, K_g^{b_{4,i,j}}\, t_s^{b_{5,i,j}}) x R_{2D} \qquad (12)$$

However, as the distance, d_c has no effect on the maximum shear force, it is not included in the developed equation. The coefficients, $a_{i,j}$, $b_{1,i,j}$, $b_{2,i,j}$, $b_{3,i,j}$, $b_{4,i,j}$ and $b_{5,i,j}$ in Eq. 12 are given in Table 5.3. for the cases of one, two, three and four girders on the cantilever part of the cap beam. The girder live load reaction forces calculated from Eq. 12 are substituted in Eq. 4 to calculate the maximum shear force and in Eq. 5 to calculate the accompanying moment in the cap beam.

Table 5.3. *Coefficients for Eq. 12 to calculate the maximum column face shear forces, Nc: number of girders resting on the cantilever part of the beam*

N_c	i	$a_{i,j}$	$b_{1,i,j}$	$b_{2,i,j}$	$b_{3,i,j}$	$b_{4,i,j}$	$b_{5,i,j}$
1	1	1.15	-0.33	0.5	0.25	-0.05	0.04
2	1	0.75	-0.15	0.4	0.25	-0.1	0.15
	2	0.28	-0.03	0.9	-0.03	0.06	-0.2
3	1	0.5	-0.01	0.3	0.2	-0.1	0.15
	2	0.2	0.3	0.7	-0.02	0.05	-0.1
	3	0.2	0.2	0.6	-0.03	0.025	-0.06
4	1	0.25	0.15	0.25	0.25	-0.1	0.1
	2	0.3	0.05	0.6	-0.01	0.02	-0.07
	3	0.3	0.02	0.7	-0.01	0.02	-0.04
	4	0.15	0.1	1	-0.01	-0.004	-0.02

5.2.2. Design Equations for Pier Column and Foundation Design

In the case of the hammer-head pier column, the live load does not create any shear force (Figure 5.1.). Accordingly, for the design of the column and the foundation, the maximum column base moment (column top moment is also equal to the column base moment) with accompanying column axial load and the maximum column axial load with accompanying column base moment are needed.

5.2.2.1. Equations to Calculate the Maximum Column Axial Load and Accompanying Moment

The parametric analyses results revealed that the maximum axial load in the column occurs when all the lanes are loaded. Therefore, from the static equilibrium point of view, the maximum axial load, $N_{C\text{-}Max}$ is equal to the live load reaction force from 2D analysis (only one lane loaded) multiplied by the total number of design lanes, n_l and the multiple presence factor, *mpf*, as follows;

$$N_{C-Max} = mpf\ n_l\ R_{2D} \tag{13}$$

However, for the moment, M_C, accompanying the maximum column axial load, there may be several alternatives depending on the position of the trucks across the bridge width. As the transverse load configuration where the first truck is located closest to

the edge of the bridge creates the largest moment, this moment is used as M_C. Accordingly, the difference, w_l, between the bridge width, w and the total width formed by the trucks placed side-by-side (distance between the left wheel of the leftmost truck and right wheel of the rightmost truck (Figure 2.2.) becomes an important parameter affecting the value of M_C and it is included in the regression analyses together with the significant parameters found from sensitivity analyses. The parameter w_l, is calculated as;

$$w_l = w - [1.8\,x\,n_l + 1.2\,x\,(n_l - 1)] = w - (3n_l - 1.2) \qquad (14)$$

A regression analysis procedure similar to that described earlier is followed to formulate M_C. However, in this specific case, the regression analyses are directly performed on M_C rather than the girder live load support reactions, since a direct formulation of M_C produced results in good agreement with those of the FEM analyses. The formulated equation for M_C is as follows;

$$M_c = (0.034\,NS^{0.86} w_l^{1.6}\,(d_h/S)^{0.16}\,K_g^{-0.075}\,t_s^{-0.025}) x R_{2D} \qquad (15)$$

5.2.2.2. Equations to Calculate the Maximum Column Moment and Accompanying Axial Load

An approach similar to that described above is adopted to formulate the maximum column moment, $M_{C\text{-}Max}$ and accompanying column axial load, N_C. In this specific case, however, the regression analyses results indicated that equations based on only the parameters determined by the sensitivity analyses were capable of accurately predicting the FEM results. Accordingly, the developed equations for $M_{C\text{-}Max}$ and N_C are presented in the following forms;

$$M_{C-Max} = (0.05\,N^2\,S^{1.7}\,(d_h/S)^{0.14}\,K_g^{-0.025}\,t_s^{0.01}) x R_{2D} \qquad (16)$$

$$N_C = (0.45\,N^{0.6}\,S^{0.5}\,(d_h/S)^{0.05}\,K_g^{-0.01}\,t_s^{0.02}) x R_{2D} \qquad (17)$$

CHAPTER 6

VERIFICATION OF THE PROPOSED DESIGN EQUATIONS

6.1. Verification via Using the Entire Pool of Data

To verify the accuracy of the proposed design equations, the hammer-head pier live load responses calculated using the proposed equations are compared to those from FEM analyses for a wide range of parameters. Table 6.1. presents the average of the ratios of the live load responses obtained from the proposed equations to the FEM analyses results and their standard deviation for the entire pool of data (more than 50000 data points). It is observed that while the average of the ratios range between 0.99 and 1.02, the standard deviation varies between 0.0 and 0.23 for various response ratios. The largest standard deviation (0.23) occurs for the case of the column moment accompanying the maximum column axial load, which is unlikely to govern the design of the hammer-head pier. In general, the cap beam live load responses are predicted better than those of the column. The main reason for this is that the formulation of the cap beam responses is based on the girder live load support reactions and as a result, the proposed equations for the cap beam are decoupled from the geometric properties of the hammer-head pier. On the other hand, the estimation of the maximum axial load in the column is exact as it is solely based on the principles of statics and knowing that all the lanes must be loaded to maximize the column axial load. Generally, the data presented in the table show that the proposed design equations produce reasonably good estimates of the FEM analyses results.

It is observed that while the average of the ratios range between 0.99 and 1.02, the standard deviation varies between 0.0 and 0.23 for various response ratios. The largest standard deviation (0.23) occurs for the case of the column moment accompanying the maximum column axial load, which is unlikely to govern the design of the hammer-head pier. Furthermore, the design equations for the cap beam live load responses are found to yield better estimates of the FEM analyses results compared to those of the

column. This is anticipated since an equation is proposed for each girder support reaction to calculate the maximum moment and shear in the cap beam and hence, the geometric properties of the cap beam is decoupled from the formulation.

Table 6.1. *The average ratio and standard deviation*

	Average Ratio	Standard Deviation
$M_{B\text{-}Max}$ (kN.m)	0.99	0.11
V_B (kN)	0.99	0.11
$V_{B\text{-}Max}$ (kN)	1.00	0.10
M_B (kN.m)	1.00	0.10
M_C (kN.m)	1.02	0.23
$M_{C\text{-}Max}$ (kN.m)	1.01	0.18
N_C (kN)	1.01	0.13

Furthermore, the hammer-head pier live load responses calculated using the proposed equations and those obtained from FEM analyses are compared in Figures 6.1.- 6.5. as a function of various parameters. The live load response data presented in the figures are normalized with respect to the live load support reaction obtained via 2D moving load analyses. Figure 6.1. compares the normalized maximum cap beam moments obtained from the proposed equation and FEM analyses as a function of various parameters. The figure shows a reasonably good agreement between the results of the proposed equation and the FEM analyses. Similarly, Figure 6.2. compares the normalized maximum shear forces in the cap beam. In the case of the maximum shear force, even a better agreement between the results of the proposed equation and the FEM analyses is observed. This is expected as the equation for the maximum cap beam moment involves the moment arms of the girder support reactions, which depend on the geometry of the hammer-head pier such as column width. In a similar fashion, Figure 6.3. compares the normalized maximum column moments. Also, in this case, a good agreement is found between the results of the proposed equation and the FEM analyses. In Figure 6.4., the normalized axial loads accompanying the maximum column moments are compared. The figure shows a reasonably good agreement between the results of the proposed equation and the FEM

analyses. It is noteworthy that the saw-tooth type of trend in the graphs for the number of girders and girder spacing is due to the sudden increase in the number of lanes since the bridge becomes wider as the number of girders or girder spacing increases. Figure 6.5., compares the normalized moments accompanying the maximum column axial loads. For the cases of different number of girders, a fluctuation in the magnitude of the moment accompanying the maximum column axial load is noticed. As stated earlier, the maximum axial load, $N_{C\text{-}Max}$ and the largest accompanying moment, M_C simultaneously occur when all the lanes are fully loaded and the first truck is placed nearest to the bridge edge. If the transverse configuration of the trucks is symmetrical with respect to the bridge centerline, the value of M_C becomes zero, while it increases as the eccentricity of the truck configuration with respect to the bridge centerline increases. In the design equation (Eq. 15), this phenomenon is taken into consideration with the introduction of w_l as a parameter. Generally, while the proposed equation produces estimates of M_C in good agreement with the FEM analyses results, a slight overestimation is observed.

It is noteworthy that the comparisons of the normalized responses are deliberately performed for the cases where the difference between the results of the proposed equations and FEM analyses are relatively more exaggerated. Furthermore, it is observed that in most cases the proposed equations yield slightly more conservative estimates of the live load responses. However, in general the comparison of the results of FEM analyses and proposed equations shows that the proposed design equations are in compliance with the FEM results for a wide range of the values of parameters considered in this study, thus demonstrating their reasonably good accuracy and reliability.

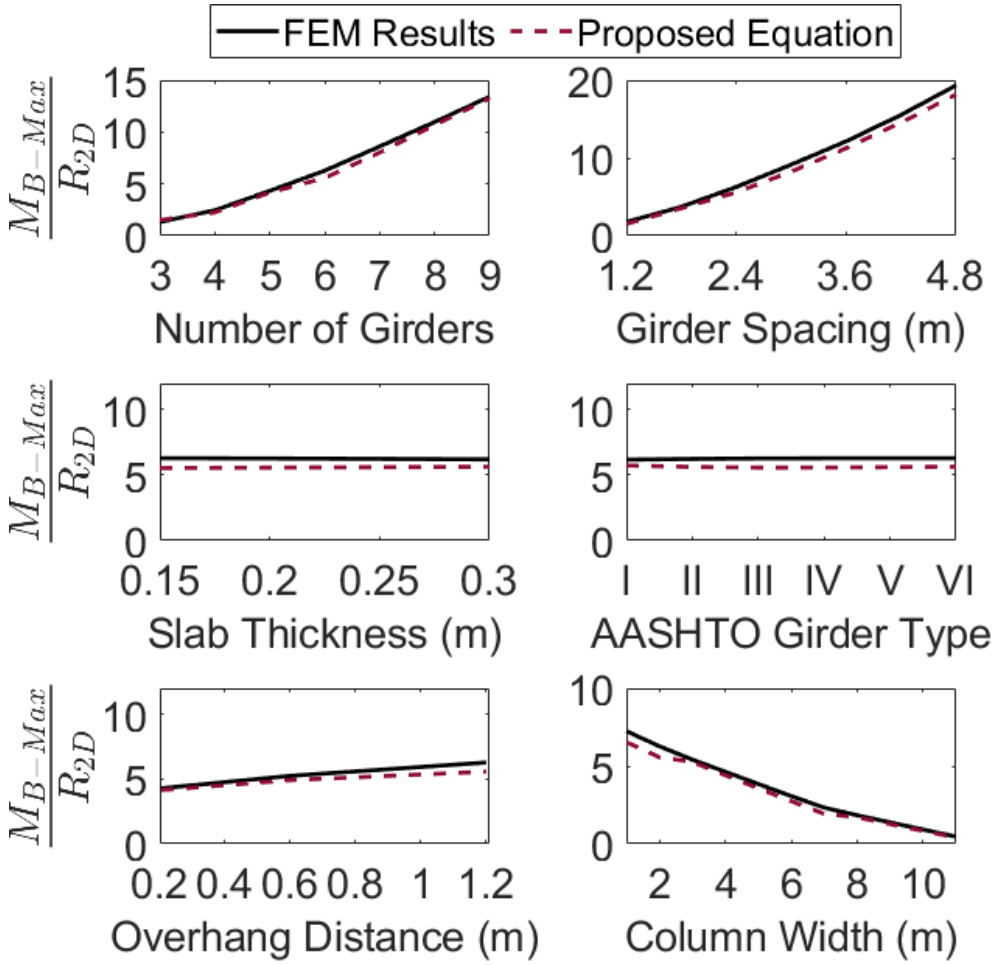

Figure 6.1. Comparison of FEM results and proposed equation for $M_{B\text{-}Max}$ / R_{2D} as a function of various parameters (Number of girders = 6, AASHTO Type III girder, S = 2.4 m, d_e = 1.2 m, column width = 2.0 m, t_s = 0.20 m)

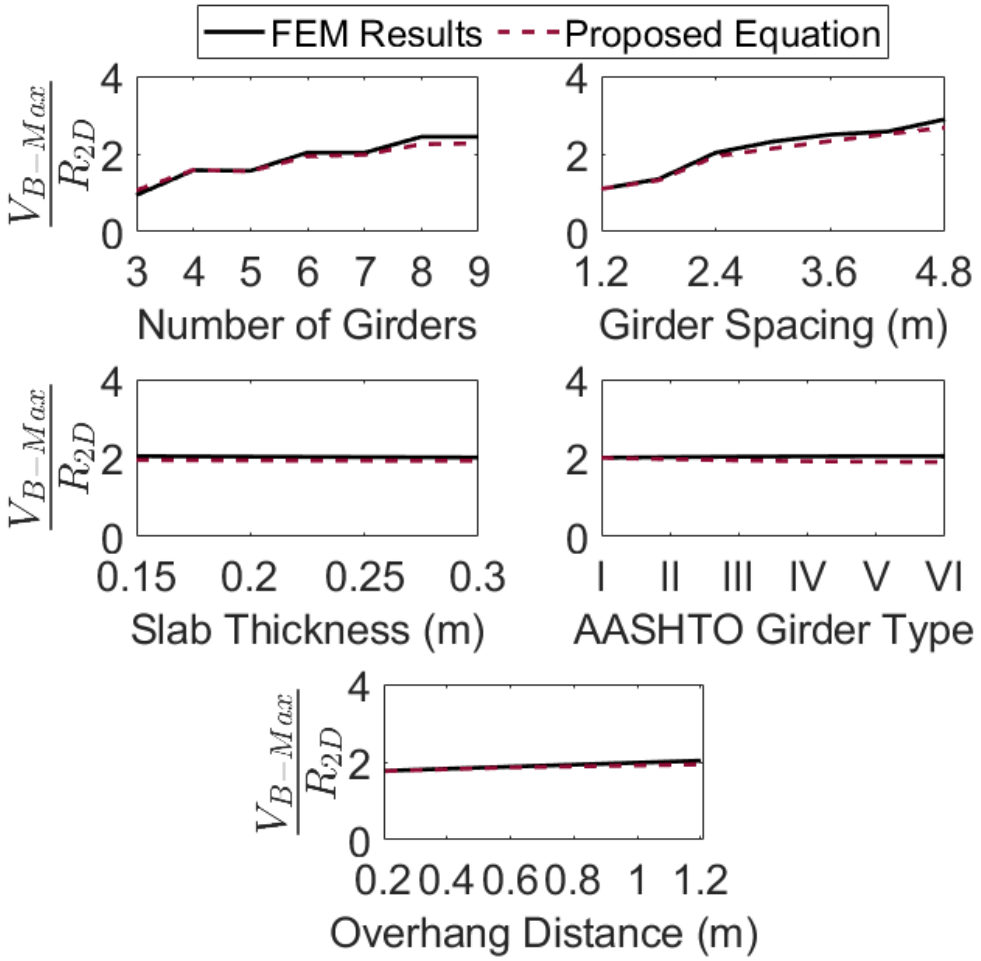

Figure 6.2. **.** Comparison of FEM results and proposed equation for $V_{B\text{-}Max}$ / R_{2D} as a function of various parameters (Number of girders = 6, AASHTO Type III girder, S = 2.4 m, d_e = 1.2 m, column width = 2.0 m, t_s = 0.20 m)

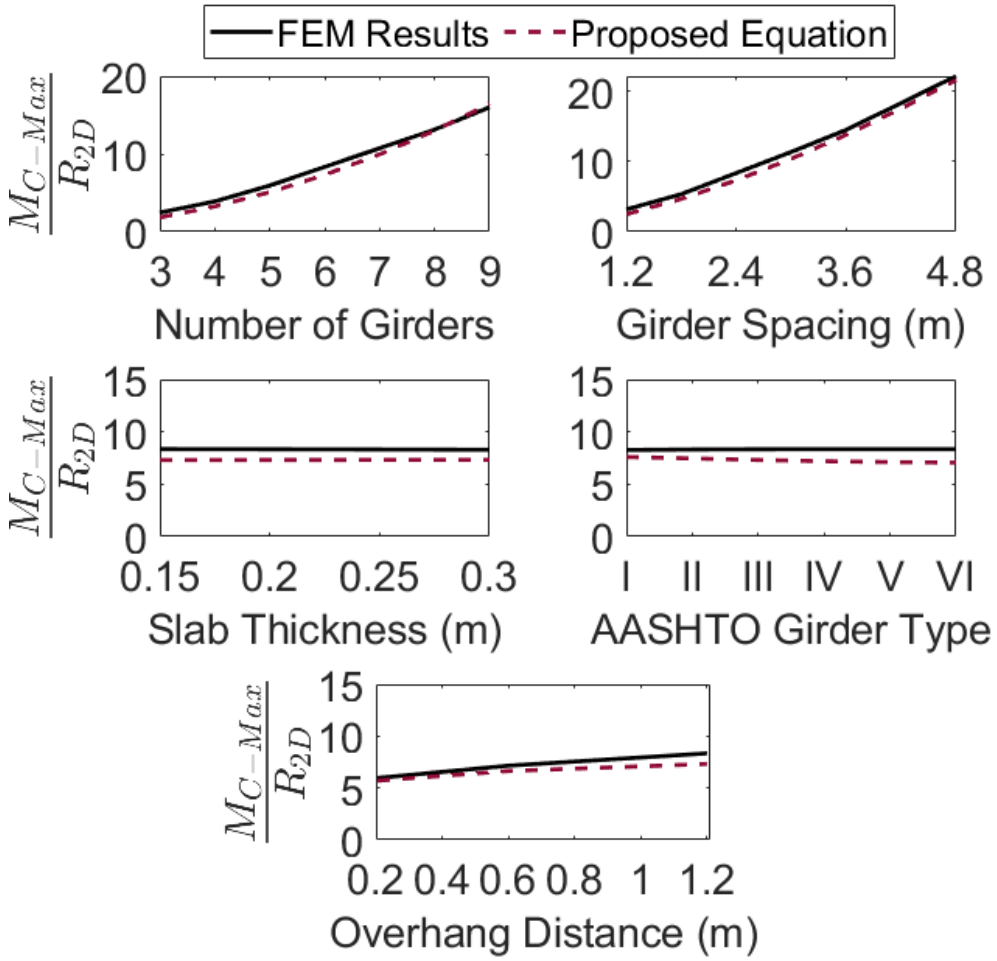

Figure 6.3. *Comparison of FEM results and proposed equation for $M_{c\text{-}Max}$ / R_{2D} as a function of various parameters (Number of girders = 6, AASHTO Type III girder, S = 2.4 m, d_e = 1.2 m, column width = 2.0 m, t_s = 0.20 m)*

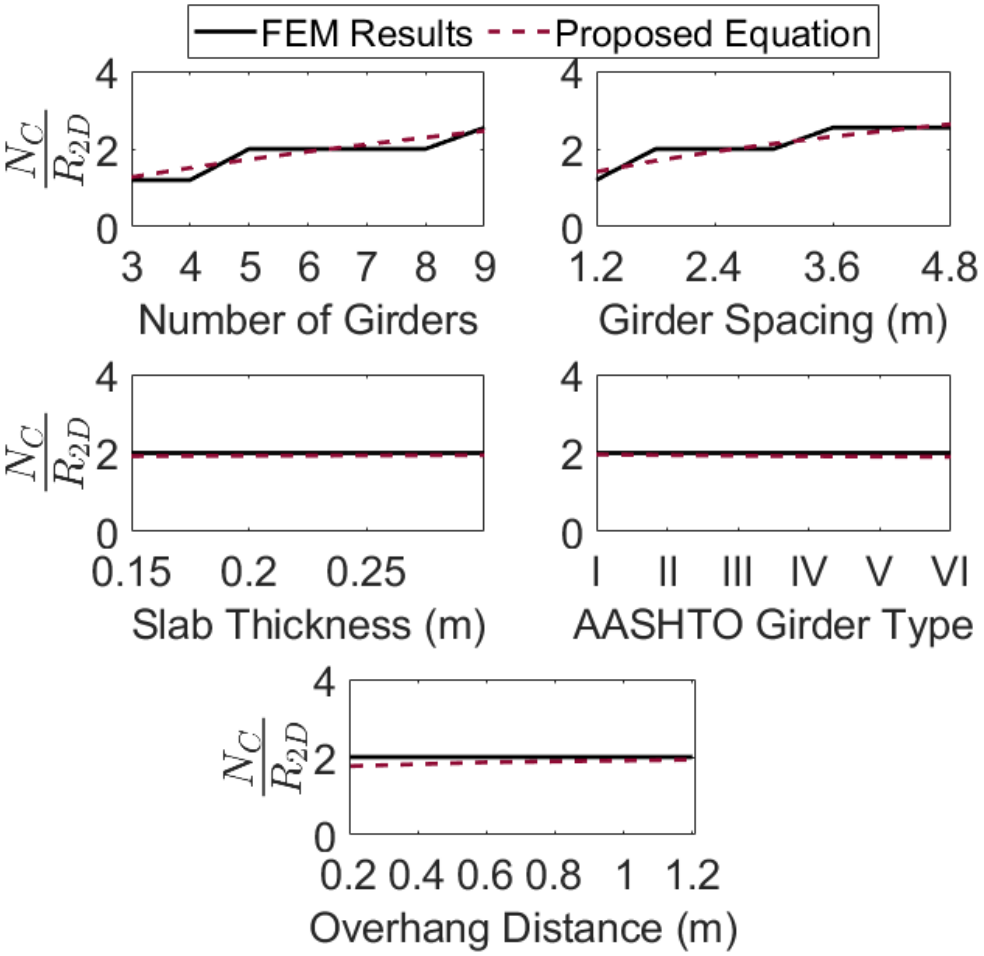

Figure 6.4. Comparison of FEM results and proposed equation for N_c / R_{2D} as a function of various parameters (Number of girders = 6, AASHTO Type III girder, S = 2.4 m, d_e = 1.2 m, column width = 2.0 m, t_s = 0.20 m)

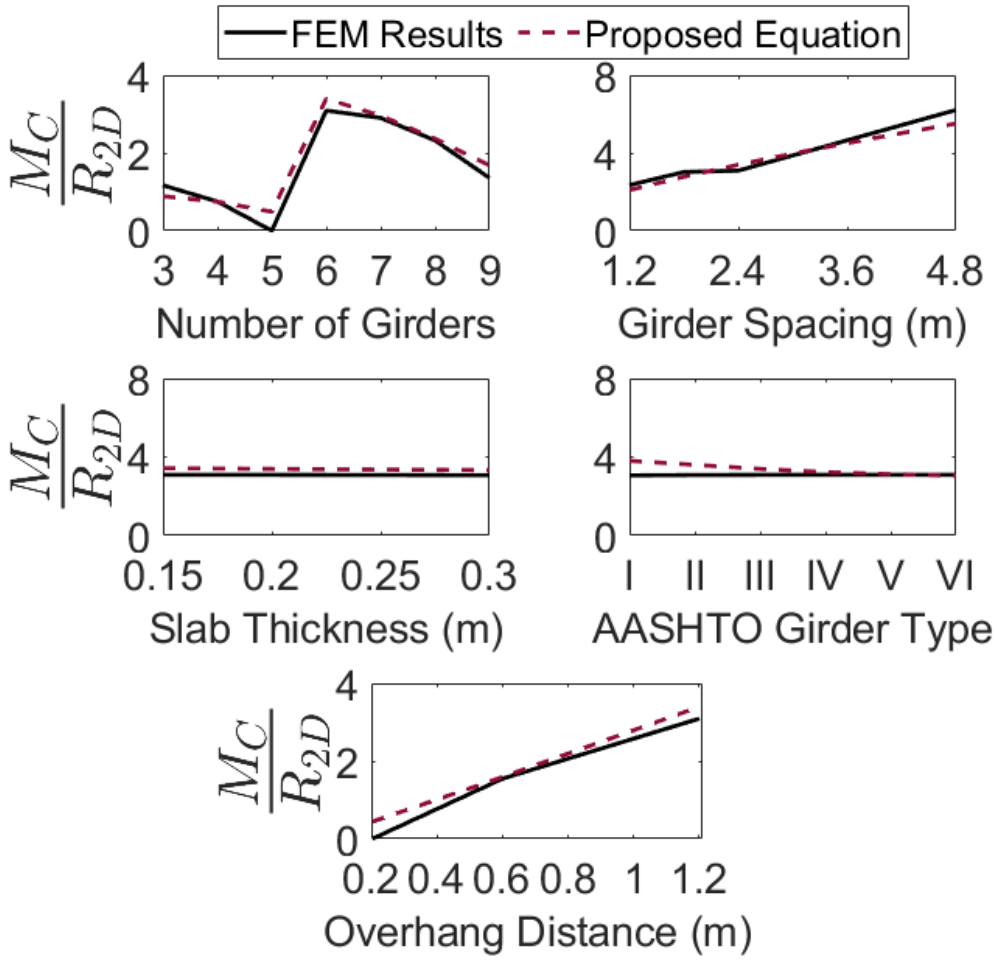

Figure 6.5. Comparison of FEM results and proposed equation for M_c / R_{2D} as a function of various parameters (Number of girders = 6, AASHTO Type III girder, S = 2.4 m, de = 1.2 m, column width = 2.0 m, ts = 0.20 m)

6.2. Verification via Realistic Case Studies of Bridges

To further verify the proposed design equations, the FEMs of two bridges with properties given in Table 6.2. are built and analyzed. In both bridge models, lane loading along with the HL-93 truck as described in AASHTO (2017) are applied. The dynamic allowance factor is also included for the HL-93 truck and multiple presence factors are considered to reflect a real bridge design scenario. The FEM analysis results and those obtained using the proposed equations are presented in the Table 6.3. for various hammer-head pier responses. The results in Table 6.3. reveal that the proposed design equations yield hammer-head pier responses comparable to those from FEM analyses.

Table 6.2. *Test bridge model parameters (w_c = column width in meters)*

Test Bridge	L (m)	Number of Girders	S (m)	t_s (m)	Girder Type	d_h (m)	w_c (m)
1	15	6	3.0	0.25	AASHTO Girder Type I	1.2	5
2	45	8	1.8	0.25	AASHTO Girder Type VI	0.6	5

Table 6.3. *Comparison of FEM analysis results with design equations results*

	Test Model 1			Test Model 2		
	Design Equations	FEM Analyses	Ratio	Design Equations	FEM Analyses	Ratio
$M_{B\text{-}Max}$ (kN.m)	4022	3724	1.08	4220	4041	1.04
$V_{B\text{-}Max}$ (kN)	1029	1051	0.98	1999	1932	1.03
M_C (kN.m)	2552	2248	1.14	2655	2790	0.95
$M_{C\text{-}Max}$ (kN.m)	6243	6578	0.95	8763	9312	0.94
N_C (kN)	1262	1159	1.09	2321	2407	0.96

CHAPTER 7

CONCLUSIONS

In this study, parametric analyses are conducted to obtain design equations to estimate live load effects in hammer-head bridge piers. FEM of a benchmark bridge is built, and sensitivity analyses are performed on the bridge model to identify the bridge parameters affecting the magnitude and distribution of the girder live load support reactions and hence the internal forces in the hammer-head pier components. Followings are the important observations from sensitivity analyses:

- The sensitivity analyses results revealed that the piers need not be included in the FEM of the bridge for estimating the girder live load support reactions.

- The girder spacing is found to affect the distribution of girder live load support reactions. This is anticipated since the truck wheel loads are distributed by the bending rigidity of the slab between the girders and hence one may expect a better distribution of the load as the girder spacing decreases.

- The girder rigidity is also found to affect the distribution of girder live load support reactions. This is expected as the bending of more flexible girders forces the truck wheel loads further away from the pier supports to be distributed to the adjacent girders. This results in a better distribution of the wheel loads to the supports.

- The effect of the number of girders on the distribution of girder live load support reactions is found to be notable. This is expected since as the number of girders increases the live load is distributed over more girders.

- The number of spans in a bridge is found to have only a negligible effect on the distribution of girder live load support reactions. Although the total reaction forces over the piers may be different, the distribution of these reaction forces among the girders is nearly independent of the number of spans. That is, the girder reaction forces

normalized with respect to the total reaction force over the pier is similar for all the piers.

- It is observed that there is a significant discrepancy as much as 51% between the maximum girder reaction forces as a function of the overhang distance. Such a large discrepancy is expected since the overhang part of the slab is a cantilever structure affecting the position of the truck wheel load with respect to the exterior girder, and hence the distribution of the total live load among the girder supports.

- The sensitivity analyses results reveal that especially for smaller number of loaded design lanes, there is a discrepancy as much as 10% in the maximum girder reaction forces as a function of the slab thickness. This is expected since a better distribution of live load among the girders is anticipated for stiffer slabs.

- The span length is found not to have any effect on the distribution of girder live load support reactions. The span length may normally affect the magnitude of the total live load reaction force over the pier. However, the variation in the distribution of this total reaction force among the girder supports for different span lengths is negligible.

Following the sensitivity analyses, parametric analyses of bridges are performed where each parameter is assigned a wide range of values. Subsequently, minimum least squares regression analyses of more than 50000 data is performed to obtain equations to estimate the maximum cap beam moment and shear force, the maximum column moment and accompanying axial load as well as the maximum column axial load and accompanying moment. Then, the average of the ratios of the live load responses obtained from the proposed equations to the FEM analyses results and their standard deviation for the entire pool of data (more than 50000 data points) are calculated. It is observed that while the average of the ratios range between 0.99 and 1.02, the standard deviation varies between 0.0 and 0.23 for various response ratios. The largest standard deviation (0.23) occurs for the case of the column moment accompanying the maximum column axial load, which is unlikely to govern the design

of the hammer-head pier. Furthermore, the design equations for the cap beam live load responses are found to yield better estimates of the FEM analyses results compared to those of the column. This is anticipated since an equation is proposed for each girder support reaction to calculate the maximum moment and shear in the cap beam and hence, the geometric properties of the cap beam is decoupled from the formulation.

For further verification of the proposed design equations, the FEMs of two test bridges with different properties are built and analyzed. The comparison of the FEM analysis results of both bridges with those from the proposed design equations revealed that the proposed design equations yield comparable results to those of the FEM analyses. Accordingly, the proposed design equations may be used in practice for the design of hammer-head bridge piers to avoid complicated finite element modeling and analyses of bridges.

REFERENCES

American Association of State Highway and Transportation Officials, (AASHTO). LRFD Bridge Design Specifications, 8th Ed., Washington, D.C., 2017.

Barr, P. J., Eberhard, M. O., Stanton, J. F. Live-Load Distribution Factors in Prestressed Concrete Girder Bridges, Journal of Bridge Engineering, 6(5), 298-306, 2001.

Cai, C. S. Discussion on AASHTO LRFD Load Distribution Factors for Slab-on-Girder Bridges, Practice Periodical on Structural Design and Construction, 10(3), 171-176, 2005.

Dicleli, M. and Erhan, S. Live Load Distribution Formulas for Single Span Prestressed Concrete Integral Abutment Bridge Girders, ASCE Journal of Bridge Engineering, Vol. 14, No. 6, pp. 472-486, 2009.

Erhan, S. and Dicleli, M. Live Load Distribution Equations for Integral Bridge Substructures, Engineering Structures, Elsevier Science, Vol. 31, No. 5, pp. 1250-1264, 2009a.

Erhan, S. and Dicleli, M. Investigation of the Applicability of AASHTO Live Load Distribution Equations for Integral Bridge Substructures, Advances in Structural Engineering, Multi-Science, Vol. 12, No. 4, pp. 559-578, 2009b.

Hays, C. O., Sessions, L. M., Berry, A. J. Further Studies on Lateral Load Distribution using FEA, Transportation Research Record, 1072, 1986.

Huo, X. S., Wasserman, E. P., & Iqbal, R. A. Simplified Method for Calculating Lateral Distribution Factors for Live Load Shear, Journal of Bridge Engineering, 10(5), 544-554, 2005.

Liu, R., Ji, Y., Rens, K. L. Collapses of Single Column Pier Bridges in China, In Forensic Engineering 2015 (pp. 727-735), 2015.

Lounis, Z., & Cohn, M. Z. Optimization of Precast Prestressed Concrete Bridge Girder Systems, PCI Journal, 38(4), 60-78, 1993.

Mabsout, M. E., Tarhini, K. M., Frederick, G. R., Tayar, C. Finite-Element Analysis of Steel Girder Highway Bridges, Journal of Bridge Engineering, 2(3), 83-87, 1997.

Patrick, M. D., Huo, X. S., Puckett, J. A., Jablin, M., Mertz, D. Sensitivity of Live Load Distribution Factors to Vehicle Spacing, Journal of Bridge Engineering, 11(1), 131-134, 2006.

SAP2000 Advanced 14.0.0 Computers and Structures, Inc., Berkeley, CA, USA, 2009

Wassef, W., Smith, C., Clancy, C., Smith, M. Comprehensive Design Example for Prestressed Concrete (PSC) Girder Superstructure Bridge with Commentary. Federal Highway Administration Report No. FHWA NHI-04-043, Grant No. DTFH61-02-D-63006. Washington, DC: US Government Printing Office, 2003.

Williams, M. E., Hoit, M. I. Bridge Pier Live Load Analysis Using Neural Networks, Advances in Engineering Software, 35(10-11), 645-652, 2004.

Yousif, Z., Hindi, R. AASHTO-LRFD Live Load Distribution for Beam-and-Slab Bridges: Limitations and Applicability, Journal of Bridge Engineering, 12(6), 765-773, 2007.

Zokaie, T. AASHTO-LRFD Live Load Distribution Specifications, Journal of Bridge Engineering, 5(2), 131-138, 2000.